New Views of Magnetosphere-Ionosphere Dynamics From SuperDARN Radars at Middle Latitudes

*Joseph B. H. Baker[1,2], Nozomu Nishitani[2], Pavlo V. Ponomarenko[3,2], Tomoaki Hori[2], J Michael Ruohoniemi[1]

1. Virginia Tech, 2. Nagoya University, 3. University of Saskatchewan

In recent years, capabilities for monitoring ionospheric processes in the subauroral region have been significantly improved by expansion of the Super Dual Auroral Radar Network (SuperDARN) into middle latitudes. At the present time, 13 SuperDARN radars are operational at magnetic latitudes equatorward of 55 degrees. The collective coverage area of these radars in the northern hemisphere alone spans more than 12 hours of magnetic local time. Such measurements are valuable for monitoring coupled magnetosphere-ionosphere dynamics over hemispheric spatial scales, particularly when combined with other distributed datasets, such as ground magnetometers and imagers, AMPERE Field-Aligned Currents, and GPS Total Electron Content (TEC). In this presentation, the history of SuperDARN will be briefly reviewed with a particular emphasis on the new science investigations enabled by the radars at middle latitudes. Topics covered include storm-time expansion of auroral flows, large-scale structure of the Sub-Auroral Polarization Stream (SAPS), quiet-time subauroral convection, Traveling Ionospheric Disturbances (TIDs), and mid-latitude ULF pulsations.

Keywords: SuperDARN, Ionosphere, Mid-Latitude

Dynamics of the ionospheric convection during disturbed periods observed by the mid-latitude SuperDARN radars

*Nozomu Nishitani[1], Tomoaki Hori[2], Joseph B.H. Baker[3,1]

1. Institute for Space-Earth Environmental Research, Nagoya University, 2. Graduate school of Science, University of Tokyo, 3. Virginia Tech

Sub-Auroral Polarization Streams (SAPS) are one of the main disturbance signatures in the ionospheric convection at subauroral latitudes. Their generation is related to a wide variety of factors such as ring current distribution, solar wind / magnetospheric conditions, ionospheric conductivity etc. In this paper we discuss one event of the SAPS signature observed by the SuperDARN Hokkaido East radar on April 5, 2012. Simultaneously with the enhancement / decay of the SAPS, the mid-latitude SuperDARN radars in the North America observed the corresponding intensification / weakening of the convective flows in the postmidnight sector. There is no obvious solar wind / IMF condition changes, or substorm / storm developments directly related to the convection enhancements. This suggests that the SAPS might be generated in the framework of the global convection, not triggered by a simple factor. Results of detailed discussion / interpretation will be presented.

Keywords: SuperDARN Hokkaido Pair of (HOP) radars, ionospheric convection, geomagnetically disturbed periods, Sub-Auroral Polarization Streams (SAPS)

SECS reconstruction of flow fluctuations with SuperDARN data

*Tomoaki Hori[1], Nozomu Nishitani[2], Kunihiro Keika[1], J. M. Ruohoniemi[3], Mariko Teramoto[2], Akimasa Ieda[2], Shin'ya Nakano[4], Kanako Seki[1], S. G. Shepherd[5], W. A. Bristow[6]

1. Graduate school of Science, University of Tokyo, 2. ISEE, Nagoya Univ., 3. Virginia Tech, 4. Institute of Statistical Mathematics , 5. Dartmouth College, 6. Univ. of Alaska, Fairbanks

We further analyze detailed properties of two-dimensional (2-D) structures of the ULF-like, ionospheric flow fluctuations during a short (~2 hours) break of the main phase of the March 2015 storm. Line-of-sight (LOS) Doppler velocities observed by two SuperDARN radars in the early morning sector were used to deduce the 2-D horizontal flows by means of the spherical elementary current system (SECS) expansion. Similar to results deduced by the conventional map potential technique, the SECS reconstruction shows that ionospheric plasma in the subauroral region flows primarily in the geomagnetically eastward direction before and after the period of the ULF-like fluctuations. The reconstructed flow pattern shows that, during the first half of the ULF event interval, background convection subsides and circular/elliptically polarized flow fluctuations pass over the field-of-view of the radars as they propagate westward. Multiple flow bursts likely associated with small injections occur concurrently during the second half period, while the westward-propagating flow fluctuations still continue regardless of the bursts until a major substorm activity starts later on. Some eastward-propagating flow fluctuations are seen in the early morning sector upon onset of the major substorm, which is strongly suggested by the fact that multiple injections are seen around midnight by Van Allen Probes and the SYM-H and AL indices resume growing. A new finding from the reconstructed flow then is that the eastward-propagating structures are also dominated by a poloidal component. The common feature of poloidal-dominant fluctuations implies that the westward- and subsequent eastward-propagating fluctuations are both caused by a similar mechanism.

Keywords: ionosphere, ULF, SuperDARN

Propagation and evolution of electric fields associated with solar wind pressure pulses based on spacecraft and ground-based observations

*Naoko Takahashi[1], Yasumasa Kasaba[1], Yukitoshi Nishimura[2,3], Atsuki Shinbori[4], Takashi Kikuchi[4,5], Tomoaki Hori[6], Yusuke Ebihara[5], Nozomu Nishitani[4]

1. Dep. Geophysics Graduate School of Science Tohoku University, 2. University of California, Los Angeles, 3. Boston University, 4. Institute for Space-Earth Environment Research, Nagoya University, 5. Research Institute for Sustainable Humanosphere, Kyoto University, 6. Department of Earth and Planetary Science, Graduate school of Science, The University of Tokyo

We investigate spatial and temporal evolution of large-scale electric fields in the magnetosphere and ionosphere associated with sudden commencements (SCs) using multi-point equatorial magnetospheric (THEMIS, RBSP, GOES) and ionospheric (C/NOFS) satellites with radars (SuperDARN). A distinct SC event on March 17, 2013 and a statistical analysis of 130 SC events show that the magnetospheric electric field in the equatorial plane propagates from dayside toward nightside as a compressional wave. Estimated tailward propagation speed is about 1000–1100 km/s, which can be explained by a fast mode wave. The ionospheric electric field responds ~41 s after the onset of dayside magnetospheric electric field, which can be explained by the Alfvén wave speed. Tailward and downgoing field-aligned Poynting fluxes evaluated from THEMIS and RBSP data support these propagations. We also statistically derive a spatial distribution and time evolution of the magnetospheric electric field in the dawn-dusk direction (E_y). Our result shows that negative E_y (dawnward) propagates from noon toward the magnetotail, followed by positive E_y (duskward). At noon, negative E_y lasts for about 1 min, and positive E_y becomes dominant about 2 min after the SC onset. Negative E_y soon attenuates in the nightside region, while the positive E_y propagates fairly well to the pre-midnight or post-midnight regions while maintaining a certain amplitude. The enhancement of duskward electric field is affected by the evolution of the current system associated with the main impulse of SCs.

Investigation of ion composition of the inner magnetosphere from magnetosonic wave observations

*Yoshizumi Miyoshi[1], koji nomura[1], Satoshi Kurita[1], Shoya Matsuda[1], Kunihiro Keika[2], Masafumi Shoji[1], Yoshiya Kasahara[3], Naritoshi Kitamura[4], Shinobu Machida[1], Ondrej Santolik[5], Craig Kletzing[6], Scott Boardsen[7], John Wygant[8], Richard Horne[9]

1. Institute for Space-Earth Environmental Research, Nagoya University, 2. University of Tokyo, 3. Kanazawa University, 4. JAXA, 5. CAS, 6. University of Iowa, 7. NASA, 8. University of Minesota, 9. BAS

Magnetosonic waves (MSWs) (or equatorial noise) are electromagnetic emissions whose properties can be described by the cold plasma extraordinary mode. MSWs are typically observed between the proton cyclotron frequency and the lower hybrid resonant frequency generated by the ring distributions of energetic protons. We have investigated fundamental characteristics of MSWs using the data from EFW and EMFISIS of Van Allen Probes. MSWs propagate toward the Earth, and L=0 cut off at half-proton gyro frequency are sometimes found at L<2. This suggests the existence of ions with M/Q=2, i.e., H2+ or He++ which has been confirmed by previous studies (e.g., Matsuda et al.[2016]). Since L=0 cut off and cross-over frequencies depend on the ion composition of the ambient plasma, we can derive the ion composition ratio along the satellite orbit by investigation of L=0 as well as cross-over frequencies from the Van Allen Probes data. The results show that the maximum percentage of M/Q=2 ions at L<2 is less than 10%, and the oxygen ions is a primary component at the low altitudes. This method is a good diagnostic tool to investigate quantitatively ion composition in the inner magnetosphere, which may be applicable for the data from the Arase (ERG) satellite.

Keywords: equatorial noise, ion composition, inner magnetosphere

Generation of Alfvenic Electromagnetic Plasma Structures in the M-I Coupling Auroral Current System and a Unified Mechanism of Auroral Particle Acceleration

*Yan Song[1], Robert L Lysak[1]

1. University of Minnesota

Field-aligned potential drops are most powerful to accelerate auroral particles to high energy. However, once the parallel electric fields are produced, they will disappear right away unless the electric fields can be continuously generated and sustained for a fairly long time. Thus, the generation of a long-lasting parallel electrostatic electric field is needed for the acceleration of auroral particles to high energy and for the emission of auroral kilometric radiation (AKR).

Propagation and reflection of Alfven waves in the M-I coupling auroral current system can redistribute reactive stresses, which include mechanical and magnetic stresses, along magnetic field lines, producing localized stress concentration in the auroral acceleration region. We propose that the nonlinear interaction of incident and reflected Alfven wave packets in the reactive stress concentration regions can create Alfvenic electromagnetic (EM) plasma structures in the auroral acceleration region. The Alfvenic Double Layer (DL) is one of the Alfvenic EM plasma structures which consists of localized self-sustained electrostatic electric fields associated with charge separation, which are embedded in the low density cavities and surrounded by enhanced reactive stresses. The enhanced magnetic and velocity fields carrying free energy serve as the local dynamo. The generated electrostatic electric fields will quickly deepen the seed low density cavity, which can further rapidly enhance the generation of stronger electrostatic electric fields, causing auroral particle acceleration to high energy. The Poynting flux carried by Alfven waves can continuously supply energy from the generator region to the auroral acceleration region, supporting and sustaining Alfvenic DLs and constituting a powerful long-lasting electrostatic electric field.

We suggest that the Alfvenic EM Plasma structure is a new type of fundamental dynamical EM plasma states, which can be in quasi-stationary or time-dependent. The structure acts as powerful high energy particle accelerators for the formation of quasi-static and Alfvenic auroras, and as an important source of electromagnetic radiation in cosmic plasmas.

Keywords: Dynamical Theory of Auroral Particle Acceleration, Alfvenic Electromagnetic Plasma Structures: A New Type of Fundamental Dynamical EM Plasma State, Generation of Alfvenic Double Layers by NL Interaction of Incident and Reflected Alfven Wave Packets in Auroral Acceleration Region

Magnetosphere-Ionosphere coupling process produced by Ampere force forcing from the magnetosphere

*Akimasa Yoshikawa[1]

1. Department of Earth and Planetary Sciences, Kyushu University

The way of M-I coupling process through Ampere force forcing from the magnetosphere to the ionosphere is discussed. There are many kinds of electromagnetic coupling ways between magnetosphere and ionosphere, e.g.,
1. FAC forcing: map the FAC distribution from the magnetosphere to the ionosphere and calculate ionospheric electrostatic electric field (production of FAC-free polarization field),
2. Electric field forcing: map the electric field distribution from the magnetosphere to the ionosphere and calculate the FAC distribution at the ionosphere (production of polarization-free FAC distribution).
However, as discussed by Yoshikawa et al., [2010], both of above ways cannot simultaneously satisfy energy and current conservation. Alternatively the way of M-I coupling through shear Alfven wave can do that in local coupling. On the other hand, Alfvenic-coupling with electrostatic approximation cannot provide physical mechanism how a localized Alfvenic coupling phenomenon drives global ionbospheric current system.
In this study, we propose a new way of M-I coupling theory that formulating the M-I coupling process as subsequent process of ion dynamics produced by the Ampere force forcing from the magnetosphere, that is, 3. Ampere force forcing: map the Ampere force from the magnetosphere to the ionosphere and calculate ionospheric flow through the force balance equation, induced electric field through the generalized Ohm’s law, a new magnetic field perturbation through Faraday’s induction law, new current density through Ampere’s law, and new Ampere’s force as a result of this coupling process can feed back to the magnetosphere.
Some example of M-I coupling process, aurora streamer, WTS evolution during substorm process, and dynamical Cowling channel formation will be discussed.

Keywords: Magnetosphere-Ionosphere Coupling, Ampere force forcing, dynamical polarization process

Generation of auroral turbulence in the magnetosphere-ionosphere coupling

*Tomo-Hiko Watanabe[1]

1. Graduate School of Science, Nagoya University

The magnetosphere-ionosphere (M-I) coupling is unstable to the feedback instability, when the large-scale ExB convection flow velocity exceeds a critical value, where the shear (or kinetic) Alfven waves are amplified with enhancement of the field aligned current (FAC). The local development of FAC is related to enhancement of electron precipitation and spontaneous excitation of auroral arc structures with ionospheric density increase. The feedback instability has been investigated both in the linear and the weak nonlinear regimes while the full nonlinear study is limited so far. In the present study, we discuss a nonlinear evolution of the feedback instability and transition to turbulence.
Nonlinear saturation of the feedback instability growth has recently been discussed in terms of the secondary instability [2], where the Kelvin-Helmholtz type mode is generated by a sheared ExB flow. Then, one finds transition to turbulence through the M-I coupling [2], providing a theoretical understanding on spontaneous generation of Alfvenic turbulence observed in auroral regions.

[1] T.-H. Watanabe, Phys. Plasmas 17, 022904 (2010).
[2] T.-H. Watanabe, H. Kurata, and S. Maeyama, New J. Phys. 18, 125010 (2016).

Keywords: aurora, magnetosphere-ionosphere coupling, turbulence, Alfven waves

Conjugate Observations of Electromagnetic Ion Cyclotron (EMIC) Waves Associated with Traveling Convection Vortex (TCV) Events

*Hyomin Kim[1], C. Robert Clauer[2], Andrew Gerrard[1], Mark Engebretson[3], Michael Hartinger[2], Marc Lessard[4], Juergen Matzka[5], David Sibeck[6], Howard Singer[7], Claudia Stolle[5], Daniel Weimer[2], Zhonghua Xu[2]

1. Center for Solar-Terrestrial Research, New Jersey Institute of Technology, USA, 2. Center for Space Science and Engineering Research and Department of Electrical and Computer Engineering, Virginia Tech, USA, 3. Department of Physics, Augsburg College, USA, 4. Space Science Center, University of New Hampshire, USA, 5. GFZ, German Research Centre for Geosciences, Germany, 6. NASA Goddard Space Flight Center, USA, 7. Space Weather Prediction Center, NOAA, USA

We report on simultaneous observations of EMIC waves associated with traveling convection vortex (TCV) events caused by transient solar wind dynamic pressure (Pd) impulse events. The THEMIS spacecraft located near the magnetopause observed radial fluctuations of the magnetopause and the GOES spacecraft measured sudden compression of the magnetosphere in response to sudden increases in Pd. During the transient events, EMIC waves were observed by inter-hemispheric conjugate ground-based magnetometer arrays as well as the GOES spacecraft. The spectral structures of the waves appear to be well correlated with the fluctuating motion of the magnetopause, showing compression-associated wave generation. In addition, the wave features are remarkably similar in conjugate hemispheres in terms of bandwidth, periodic wave power modulation, and polarization. Proton precipitation was also observed by the DMSP spacecraft during the wave events, from which the wave source region is estimated to be 72-74 deg in magnetic latitude, consistent with the TCV center. The confluence of space-borne and ground instruments including the the inter-hemispheric, high-latitude, fluxgate/induction-coil magnetometer array allows us to constrain the EMIC source region while also confirming the relationship between EMIC waves and the TCV current system.

Keywords: EMIC waves, Traveling Convection Vortex, Transient phenomena

Estimation of source region of pulsating proton aurora

*Tomohiro Inoue[1], Mitsunori Ozaki[2], Satoshi Yagitani[2], Kazuo Shiokawa[3], Yoshizumi Miyoshi[3], Ryuho Kataoka[4], Yusuke Ebihara[5], Reiko Nomura[6], Kaori Sakaguchi[7], Yuichi Otsuka[3], Martin G Connors[8]

1. Graduate School, Kanazawa University , 2. Institute of Science and Engineering, Kanazawa University, 3. ISEE, Nagoya University, 4. National Institute of Polar Research, 5. RISH, Kyoto University, 6. ISAS / JAXA, 7. NICT, 8. Athabasca University

Pulsating proton aurora (PPA) is caused by pitch angle scattering of high-energy (several keV ~ tens of keV) ions via the electromagnetic ion cyclotron (EMIC) waves at the magnetic equator. EMIC waves propagate along the magnetic field line from the source region and are observed as Pc1 geomagnetic pulsations on the ground. We have been investigating the source region in the magnetosphere from the traveling time difference between PPA and Pc1 geomagnetic pulsations observed on the ground. We estimated the source region using the simultaneous ground-based observations of PPA and Pc1 geomagnetic pulsations at Athabasca, Canada (L value=4.3). The PPA events were observed by using an all-sky EMCCD camera (110 Hz sampling), and the geomagnetic pulsations were measured by an induction magnetometer (64 Hz sampling). In this study, we analyzed the source region for the two events of simultaneously observed PPA and Pc1 geomagnetic pulsations on 12 November, 2015 and 2 January, 2016. The observed Pc1 geomagnetic pulsations consist of rising-tone elements having the subpacket structures. The repetition period for the rising-tone element was approximately 100 seconds. The time variation for the subpacket structures was a few tens of seconds. The PPA intensity showed the same repetition period and fast modulation. In order to estimate the source region of PPA, we calculated the time difference between PPA intensity and Pc1 amplitude taking the cross-correlation between them. The observed time difference between PPA and Pc1 geomagnetic pulsations showed that the Pc1 geomagnetic pulsations arrived at the ground station faster than the PPA. We theoretically calculated the time difference between EMIC waves and energetic ions using the group velocity of EMIC waves and the resonance energy at each magnetic latitude. The source region was estimated by comparing between the observed and theoretically calculated time differences. The estimated results showed that the source region was in the magnetic latitudes around the equator. All of the obtained results are consistent with the scenario that the high-energy ions responsible for triggering the PPA was generated at the magnetic equator.
In the presentation, we will discuss the estimation results of source regions of PPA observed at Athabasca in detail.

Keywords: Pulsating proton aurora, Pc1 geomagnetic pulsations, EMIC waves

Space-ground coordinated observations of subauroral ion drifts (SAID)

*Toshi Nishimura[1,2], Bea Gallardo-Lacourt[1], Larry Lyons[1], Eric Donovan[3], Vassilis Angelopoulos[1]

1. University of California, Los Angeles, 2. Boston University, 3. University of Calgary

Duskside plasma convection is often enhanced at narrow latitudes just equatorward of the electron auroral oval (subauroral polarization streams or SAPS). The latitudinal extent of the flows can occasionally become less than a degree with the peak speed exceeding a few km/s. Those are called subauroral ion drifts (SAID), and their formation mechanism and differences from SAPS have been key issues in subauroral magnetosphere-ionosphere coupling.

We aim at understanding occurrence timing and magnetospheric drivers of SAID by using optical imaging, radars, and low-altitude and magnetospheric satellites. Interestingly, although SAID is a subauroral phenomenon where we do not generally expect localized precipitation, all-sky imager data during a subset of SAID events showed a latitudinally narrow (~0.5 deg) auroral arc adjacent to SAID. This unique auroral feature allowed us to optically trace evolution of SAID. We found that SAID was preceded by substorm injections and SAPS, and that subsequent injections without strong proton injection resulted in SAID. This different injection behavior was confirmed by the NOAA and DMSP satellites. DMSP also showed that the bulk of the region-2 field-aligned currents (FACs) are confined to the SAID latitudinal extent. In one of the events, one of the THEMIS satellites crossed the earthward boundary of the electron plasma sheet and detected SAID with much narrower L-shell separation between electron and ion inner boundaries.

These observations indicate that SAID has a similar quasi-steady structure to SAPS both in the ionosphere and magnetosphere except for the latitudinal extent, but the type of particle injection is quite different from SAPS events; namely the injections are dominated by electrons and give much smaller separation with the ion inner boundary.

Keywords: SAPS/SAID, ring current and plasma sheet, auroral imaging and radar

Equatorial Magnetic Field of the Near-Earth Magnetotail: THEMIS Observations

*Shinichi Ohtani[1], Tetsuo Motoba[1]

1. The Johns Hopkins University Applied Physics Laboratory

The equatorial magnetic field on the night side is critical for understanding not only the configuration of the magnetotail but also its state and dynamics. The present study observationally addresses various aspects of the equatorial magnetic field such as its equatorial distribution, spatial gradient, and the occurrence of extremely weak magnetic fields using measurements made by the THEMIS satellites. An emphasis is placed on the transition region between dipolar and stretched magnetotail configurations. The results are summarized as follows: (1) within 9 R_E from Earth the magnetic field is statistically organized to a noticeable extent by the radial distance, but at a given distance it is weaker closer to midnight suggesting that it also organized by the X distance; (2) At 9-12 R_E, however, the spatial variation is less systematic suggesting that the magnetic field changes more dynamically; (3) in general, the equatorial magnetic field increases earthward steeply in the near-Earth region and far more gradually farther down the tail, and the transition takes place at $r \sim$ 9-12 R_E; (4) the gradient of the equatorial magnetic field is predominantly earthward, but it can be transiently directed tailward in association with the dipolarization of local magnetic field; (5) the equatorial magnetic field becomes extremely weak (< 2 nT) in the transition region during the substorm growth phase as well as during prolonged quiet intervals, but any clear association can be found with the steady strong driver of the magnetosphere possibly because of its rare occurrence.

Keywords: Equatorial Magnetic Field, Near-Earth Magnetotail, Plasma Sheet, Bz Minimum, Tailward Gradient of Bz, Magnetospheric Configuration

Mechanics and energetics of substorm expansion onset

*Yusuke Ebihara[1], Takashi Tanaka[2]

1. Research Institute for Sustainable Humanosphere, Kyoto University, 2. Kyushu University

Substorm expansion onset is a long-standing unsolved issue in magnetospheric. Processes taking place in the equatorial plane have been paid much attention for many years, but the connection between the equatorial plane and the ionosphere remains unclear. We focus on abrupt intensification of upward field-aligned current (FAC) that is central to this issue. That is because the upward FAC is responsible for accelerating electrons downward and emitting bright aurora and development of auroral electrojet. Here, on the basis of results of the global MHD simulation (REPPU), we show that the abrupt intensification of the upward FAC is reasonably explained by magnetohydrodynamics (MHD) processes. First of all, we focused on the magnetic field line from the onset position to the equatorial plane. The upward FAC is intensified along the magnetic field line except near the equatorial plane. The generation of the upward FAC (as a function of vorticity) takes place primarily at off-equator, not equatorial plane. The value of J.E is negative in the middle of the magnetic field line where the upward FAC is generated. This implies that the plasma moves against the Lorentz force to twist the magnetic field line and generate the FAC. These results may suggest that the abrupt intensification of the upward FAC results primarily from processes taking place at off-equator, not the equatorial plane. We will discuss the causality between the formation of the near-Earth neutral line (NENL) and the onset in terms of mechanics and energetics.

Keywords: Substorm, MHD simulation

Global MHD simulation study on substorms: Influence of low altitude boundary condition

*Naoki Kamiyoshikawa[1], Yusuke Ebihara[1], Shinichi Ohtani[2], Takashi Tanaka[3]

1. RISH, Kyoto University, 2. APL, The Johns Hopkins University, 3. SERC, Kyushu University

A substorm is one of the most drastic disturbances taking place in the magnetosphere. The substorm is known to occur frequently when the interplanetary magnetic field (IMF) is southward and solar wind speed is high. It is believed that a substorm is essentially driven by the external condition, that is, the solar wind and IMF. Recently, some simulation results have shown that the ionospheric condition may affect the global magnetospheric convection. This may imply that in addition to the external condition (solar wind and IMF), the internal condition (ionospheric condition) is also a control factor to the characteristics of substorms. We investigated the characteristics of substorms by using global magnetohydrodynamics (MHD) simulation [Tanaka et al., 2010]. For given parameters of the solar wind and IMF, we repeated the simulation by changing the inner boundary of the simulation. In the global MHD simulation, the inner boundary is located at 2.6 Re. In the original setting, plasma pressure at the innermost grid was determined by $P_1=AP_2$, where P_1 and P_2 are the plasma pressures at the lowest grid and the second lowest grid, and A is a factor. When A is 1, the plasma pressure is the same at the lowest and the second lowest grids. This means that the pressure gradient force does not exist in between. When A is less than 1, there is a pressure gradient between them, and the plasma is accelerated toward the Earth. Finally, the plasma will be lost when it encounters the innermost boundary of the simulation. In the real situation, it represents the plasma loss process due to a recombination or charge exchange in the ionosphere. We obtained the following results. For given solar wind condition, the near-Earth reconnection region as identified by earthward and tailward plasma flows occurred at ~12 Re near the equatorial plane regardless of the value *A*. However, the earthward flow speed increases with decreasing the value *A*. When the value *A* is 0.6, the earthward flow speed was about 650 km/s, whereas when the value *A* is 1.0, it was about 260 km/s. As the value *A* increases, it became clear that high-pressure regions in the near-Earth plasma sheet extended toward the Earth after the reconnection, and that the magnitude of the current density and the magnetic field before the reconnection at ~12 Re increased. In this simulation, the magnetic diffusion takes place when the anomalous resistivity is large. The anomalous resistivity is a function of the current density and the magnetic field. It is thought that the condition at the inner boundary of the simulation may change the force balance that is responsible to the anomalous resistivity and the subsequent substorm dynamics. We will discuss the detail mechanism for the dependence of *A* on the earthward-tailward flow speed as well as the magnitude of auroral electrojets and field-aligned current.

Keywords: substorm, global MHD simulation, inner magnetosphere

Response of the Earth’s magnetosphere and ionosphere to the small-scale magnetic flux rope in solar wind by the MHD simulation

*Kyung Sun Park[1], Myeong Joon Kim[1], Dae-Young Lee[1], Kyungsuk Cho[2], Rok Soon Kim[2], Tatsuki Ogino[3]

1. Chungbuk National University, Korea, 2. Korea Astronomy and Space Science Institute, Korea, 3. ISEE, Nagoya University, Japan

We have studied the response of the Earth’s magnetosphere and ionosphere to two cases of small-scale magnetic flux ropes in solar wind by using a three-dimensional global MHD simulation. (1) the case of +Z axis of magnetic flux rope, the IMF is northward with a dawn to dusk B_Y components as right-handed, (2) the case of +Y axis of magnetic flux rope, the IMF is north to southward with a duskward B_Y as right-handed and solar wind dynamic pressure is normal (1.3 nPa).
The simulation results show that the bow shock is located at about 14.6 R_E and the magnetopause is located at about 10.24 R_E in both cases. However, ionospheric phenomena show the different feature for two cases. The cross polar cap potential becomes small during the northward even though magnitude of magnetic field becomes large for +Z axis of magnetic flux rope. And the cross polar cap potential increase that is governed by magnitude of magnetic field as well as southward B_Z for +Y axis of magnetic flux rope.

Keywords: small-scale magnetic flux rope, magnetosphere and ionosphere , cross polar cap potential

Dayside plasma blob: a different high-density structure from patches in the polar cap

*Qing-He Zhang[1], Yu-Zhang Ma[1], P. T. JAYACHANDRAN[2], J. Moen[3], M. Lockwood[4], Yong-Liang Zhang[5], Yong Wang[1], D. R. Themens[2]

1. Institute of Space Sciences, Shandong University, Weihai, China, 2. Physics Department, University of New Brunswick, Fredericton, New Brunswick, Canada, 3. Department of Physics, University of Oslo, Blindern, Oslo, Norway, 4. Department of Meteorology, University of Reading, Earley Gate, Post Office Box 243, RG6 6BB, UK., 5. The Johns Hopkins University Applied Physics Laboratory, Laurel, Maryland, USA

A new nomenclature of “dayside plasma blob/dayside blob” has been introduced to differentiate another type of enhanced density structures from polar cap patches in the polar ionosphere based on the *in situ* and ground based observations, by learning from the terminology of auroral blob, a plasma structure within the night-time auroral oval on the closed field lines. Comparing with the polar cap patches, which transported from dayside sunlit region with dense and cold plasma, the dayside blobs are associated with particle precipitations and aurora arcs in the polar cap with dense and hot plasma and strong field-aligned current. Notably, the dayside blobs cause more severe disturbances in the polar cap ionosphere for navigation signals than patches, which will be very useful to grade the importance of space weather phenomena in the polar cap.

Keywords: Polar cap patches, Dayside plasma blobs, Polar Ionosphere, Polar ionosphere-magnetosphere coupling

Spatiotemporal variations of the electron precipitation producing moving cusp aurora

*Satoshi Taguchi[1], Keisuke Hosokawa[2], Yasunobu Ogawa[3]

1. Department of Geophysics, Graduate School of Science, Kyoto University, 2. Department of Communication Engineering and Informatics, University of Electro-Communications, 3. National Institute of Polar Research

A moving mesoscale aurora at a wavelength of 630.0 nm (red line) is a typical phenomenon in the dayside cusp of the high-latitude ionosphere and is thought to be caused by enhanced fluxes of soft magnetosheath electrons in the moving flux tube driven by intermittent reconnection. In this paper we examine the spatiotemporal variations of the electron precipitation in the moving reconnected flux tube by analyzing red-line aurora image data from a ground-based all-sky imager. An analysis taking into account a long radiative time of red-line emission was performed. The long radiative time is the dominant cause of the difference between the extent of the moving red-line aurora and that of the moving electron precipitation. Estimating this difference quantitatively in the aurora image obtained at a time resolution of approximately 10 s reveals the dynamic features of the electron precipitation in the moving reconnected flux tube.

Keywords: Aurora, cusp, electron precipitation

The Earth's Magnetopause: Force Balance and Topology Revealed by High Cadence Plasma Measurements

*Christopher T Russell[1], Robert J Strangeway[1], Cong Zhao[1], Brian J Anderson[2], Wolfgang Baumjohann[3], Kenneth R Bromund[4], James A Slavin[5], Larry Kepko[4,6], Guan Le[4], Werner Magnes[3], Rumi Nakamura[3], Roy B Torbert[6], William R Paterson[4], Thomas E Moore[4], Barbara L Giles[4], Stephen A Fuselier[7], James L Burch[7]

1. Earth Planetary and Space Sciences, University of California, Los Angeles, CA 90095, USA., 2. Johns Hopkins University Applied Physics Laboratory, Laurel, MD 20723-6099, USA, 3. Space Research Institute, Austrian Academy of Sciences, Graz, Austria, 4. NASA Goddard Space Flight Center, Greenbelt, MD 20771, USA, 5. University of Michigan, Climate and Space Sciences and Engineering, Ann Arbor, MI 48109-2143, USA, 6. University of New Hampshire, Durham, NH 03824, USA, 7. Southwest Research Institute, Boulder, CO 80302, USA.

The magnetopause is strongly influenced by properties of the flowing plasma that it deflects. The Magnetospheric Multiscale Mission has enabled this interaction to be probed in intimate detail. We combine the magnetic measurements of the four spacecraft to demonstrate how the magnetic forces affect the boundary between the shocked solar wind and the Earth's magnetic field. We compare these forces with the plasma pressure, confirming the accurate intercalibration of the plasma and magnetic forces but draw attention to the tradeoff between spatial resolution and accuracy of the gradient measurements so governed by the spacecraft separation. We use the electron distribution function to examine the topology of the magnetic field. Small pockets of low magnetic field strength, small radius of curvature magnetic field lines and high electric current mark the electron diffusion region.

Keywords: Magnetopause, Reconnection, Topology

The azimuthal extent of magnetopause reconnection

*Ying Zou[1], Brian Walsh[1], Toshi Nishimura[1,2], Vassilis Angelopoulos[2], John Micheal Ruohoniemi[3], Kathryn McWilliams[4], Nozomu Nishitani[5]

1. Boston Univeristy, 2. University of California Los Angeles, 3. Virginia Tech, 4. University of Saskatchewan, 5. Nagoya University

Although the dayside magnetopause reconnection is shown to occur in localized regions or over an extended X-line, a systematic understanding of what is the prevailing scale size and how this depends on IMF conditions has not been achieved. Multi-point observations by spacecraft tend to be separated either too small to cover the reconnection site, or too large that the assumption of a continuous X-line between satellites becomes questionable. Radars and imagers can broadly monitor the ionospheric signatures of magnetopause reconnection around the cusp as fast anti-sunward flows and auroras, and can thus provide a large-scale context of the reconnection scale size given by the flow channel size. We combine multi-point THEMIS spacecraft observations with SuperDARN measurements to statistically determine the width of magnetopause reconnection and its IMF dependence. We require nearly simultaneous magnetopause crossing by at least two spacecraft and determine the occurrence of reconnection based on the Walen test and the D-shape distribution of ion phase space density. This is compared with the occurrence and the azimuthal width of ionospheric fast flows at the spacecraft footprint. Our preliminary results show that when the two spacecraft are separated by a few Re and both detect reconnection signatures, their footprints are located within or close to the same ionospheric flow channel. When one misses reconnection, its footprint is located away from the ionospheric flow channel. Such conjunctions ensure the physical connection between ionospheric flow channels and magnetopause reconnection extents, and thus enable a reliable interpretation of the reconnection width. We observe the reconnection width to be 200-600 km in ionosphere, which corresponds to 2 Re up to 8 Re in the equatorial plane, although more events are under survey.

Keywords: Magnetopause reconnection, Multi-point observation, Magnetosphere-ionosphere conjunction

Seasonal and solar wind control of the reconnection line location at the Earth's dayside magnetopause

*Yasuto Hoshi[1,2], Hiroshi Hasegawa[2], Naritoshi Kitamura[2], Yoshifumi Saito[2]

1. Graduate School of Science, The University of Tokyo, 2. ISAS/JAXA

Geomagnetic disturbances in the geospace such as aurora and geomagnetic storm are driven by solar wind energy transported into the Earth's magnetosphere. Magnetic reconnection at the dayside magnetopause is the most important process by which solar wind energy enters the magnetosphere. This is a phenomenon in which the interplanetary magnetic field (IMF) in the solar wind and the Earth's magnetic field re-connect. Under southward and/or predominantly dawn-dusk IMF conditions, magnetic reconnection takes place along an extended reconnection line at low latitudes, called the X-line. Geomagnetic flux connected to the IMF is transported to, and is stored in, the nightside magnetosphere. The amount of solar wind energy that flows into the magnetosphere is controlled by the efficiency of reconnection occurring at the dayside magnetopause. The efficiency of reconnection may depend on the X-line location. When the X-line location shifts from the subsolar point, where the sun is at the zenith, the boundary conditions around the X-line can change. Therefore, the amount of solar wind energy flowing into the Earth's magnetosphere can change because of the changed efficiency of the reconnection. In recent years, some models and observations showed that finite dipole tilt or IMF B_X controls the X-line location by moving it northward or southward from the subsolar point. Although the X-line location is an important parameter in solar wind energy transport, its dependence on dipole tilt and IMF Bx is not yet made clear based on statistical observational studies. We statistically estimated the X-line location by investigating the occurrence pattern of reconnection jets observed at the dayside magnetopause. Used here are plasma and magnetic field data taken in the dayside magnetopause region within the magnetic local time range of 10 to 14 hours from 10 years of observations by the THEMIS spacecraft.

Among full magnetopause crossing events, flows with a speed tangential to the magnetopause exceeding 150 km/s, which is of the order of the Alfvén speed in the magnetosheath, are chosen as candidates of the reconnection jets. The Walén relation is used to test whether the flow was generated by reconnection, and a total of 715 jets were identified. We estimated the X-line location by the direction and position of the identified jets. The present analysis assume that the northward jets are observed on the northern side of the X-line and the southward jets are observed on the southern side. The average X-line location was estimated by determining a linear discriminant function that minimizes the occurrence probability of the southward jets on the northern side of the estimated X-line or the northward jets on the southern side. It was found that the X-line location shifts about 6 Earth radii from the subsolar point toward the winter hemisphere under the largest dipole tilt. This is also the first study that reveals that the X-line location shifts about 2.5 Earth radii from the subsolar point when the IMF B_X component is large. The results demonstrate that the effect of dipole tilt on the X-line position is larger than that of the IMF B_X component. To summarize, the dipole tilt dependence of the X-line location suggests that efficiency of energy transport into the magnetosphere by dayside magnetic reconnection during southward IMF may decrease when the dipole tilt is large. This suggests that the well-known geomagnetic activity decrease under larger dipole tilts may be partially due to the X line position displaced from the subsolar point for large dipole tilt.

Keywords: magnetopause, magnetic reconnection

Subsidence of Ionospheric Fast Flows Triggered by Magnetotail Magnetic Reconnection During Transpolar Arc Brightening

*Motoharu Nowada[1], Robert C. Fear[2], Adrian Grocott[3], Quan-Qi Shi[1], Chun-Feng Zhang[1], Yong-Fu Wang[4], Qiu-Gang Zong[4], Yong Wei[5], Sui-Yan Fu[4], Zu-Yin Pu[4]

1. Center for Space Weather Sciences, Institute of Space Science, School of Space Science and Physics, Shandong University at Weihai, 2. Department of Physics and Astronomy, University of Southampton, 3. Space and Planetary Physics Group, Department of Physics, Lancaster University , 4. Institute of Space Physics and Applied Technology, School of Earth and Space Sciences, Peking University , 5. Key Laboratory of Earth and Planetary Physics, Institute of Geology and Geophysics, Chinese Academy of Sciences

A static transpolar arc (TPA), which extended from post-midnight to pre-noon, was seen on 16th September 2001 in the northern hemisphere. The orientations of the Interplanetary Magnetic Field-B_z and -B_y components were dominantly northward and weakly dawnward, respectively, when the TPA began to brighten. Associated solar wind velocity, density and dynamic pressure were almost stable. The SuperDARN radars detected westward plasma flows whose range was between 0.4 km/s and 0.75 km/s along the poleward edge of the midnight-sector main auroral oval, suggesting that they were confined within closed field lines and identified as the ionospheric plasma flows associated with Tail Reconnection during IMF Northward Non-substorm Intervals (TRINNIs). These TRINNIs' ionospheric fast plasma flows persisted for at least 50 minutes prior to an appearance of the TPA. Often, TRINNIs are observed even during the period when the TPA is present, but, in this case, the flows associated with TRINNIs subsided beforehand. Additional slower plasma flows, which might cross the open/closed polar cap boundary, were seen at the time of the TPA onset in the same magnetic local time sector as the nightside end of the TPA. These ionospheric flows suggest that magnetotail reconnection significantly contributed to the TPA formation, which is proposed by Milan et al. [2005]. We investigate how magnetotail reconnection actually occurred before and during the TPA appearance by calculating the Joule heating (E・J) based on a global MHD simulation. Evidence for heating associated with magnetotail reconnection was seen during an interval of TRINNIs' fast flows on the midnight-sector main auroral oval prior to the TPA appearance, but no significant Joule heating due to nightside magnetic reconnection was found during the TPA brightening. This result suggests that the fate (absence or presence) of the TRINNIs' fast flows on closed field lines (the midnight-sector main auroral oval) during the TPA brightening would depend on a scale of magnetic reconnection, that is, the width of the reconnection line.

Reference:
Milan, S. E., B. Hubert, and A. Grocott (2005), Formation and motion of a transpolar arc in response to dayside and nightside reconnection, J. Geophys. Res., 110, A01212, doi:10.1029/2004JA010835.

Keywords: Transpolar Arc, Magnetotail Reconnections, Ionospheric Flows, TRINNIs

Simultaneous observation of auroral substorm onset in Polar satellite global images and ground-based all-sky images

*Akimasa Ieda[1], Kirsti Kauristie[2], Yukitoshi Nishimura[3], Yukinaga Miyashita[1], Shinobu Machida[1], Yoshizumi Miyoshi[1], George K. Parks[4], Matthew O. Fillingim[4], Kawashima Takahiro[1], Miura Tsubasa[1]

1. Institute for Space-Earth Environmental Research, Nagoya University, 2. Finnish Meteorological Institute, 3. University of California, Los Angeles, 4. University of California, Berkeley

Substorm onsets have originally been defined as longitudinally extended sudden auroral brightening ("Akasofu initial brightening") followed a few minutes later by auroral poleward expansion in ground-based all-sky images. In satellite global images, in contrast, such a clearly marked two-stage development has not been observed, and instead substorms have often appeared to start in a localized area. To resolve these differences, optical substorm onset signatures in global images and all-sky images were compared for a substorm that occurred on 7 December 1999. We have used the Polar satellite ultraviolet global images with a fixed filter (170 nm), enabling a high time resolution (37 s), and have used the 20 s resolution green line (557.7 nm) all-sky images at Muonio in Finland for comparison.

We first identified the substorm onset brightening at 2127:49 UT in the global images and then searched for corresponding signatures in the all-sky images. The Akasofu initial brightening (2124:50 UT) and the poleward expansion (2127:50 UT) were observed in the all-sky images, indicating that the onset in global images was not simultaneous with the actual onset but rather with the poleward expansion in the all-sky images. The Akasofu initial brightening was not observed in the global images, which may possibly be attributed to the limited sensitivity of global images for thin auroral arc brightenings. This result suggests that substorm onset identified in global images does not necessarily represent the Akasofu substorm onset, but rather corresponds to the poleward expansion a few minutes later.

Keywords: substorm, auroral breakup, aurora, global image, all-sky image

Study on Effects of Ionospheric Polarization Field and Inner Boundary Conditions on Magnetospheric Dynamics and Substorm Processes in Global MHD Simulation

*Aoi Nakamizo[1], Akimasa Yoshikawa[2,3], Takashi Tanaka[3]

1. Applied Electromagnetic Research Institute, National Institute of Information and Communications Technology, 2. Faculty of Science, Kyushu University, 3. International Center for Space Weather Science and Education (ICSWSE)

Global MHD simulation is an effective way to investigate the Solar Wind-Magnetosphere-Ionosphere system. Among various handlings and parameterizations in the global simulations, they are related to processes which cannot be described by MHD or which have not been fully understood, we especially place importance on the descriptions for low-altitude region (the M-I coupling part and inner boundary conditions) and we expect that they largely control the dynamics of the M-I system. In order to advance our physical understanding of the M-I system from the viewpoints of the above interests, we investigate the responses of magnetosphere and substorm processes for different treatments of low-altitude region.

Our investigation is generally classified into two categories; (A) the one in the context of the M-I coupling algorithm and (B) the other in the context of the inner boundary conditions imposed on MHD variables.
As for (A), the currently and commonly used algorithm is as follows; the FACs (rotB) of the MHD region are inputted to a potential solver embedded at the ionosphere altitude with prescribed conductance distribution, then calculated electric field is mapped back to the MHD region as the velocity field. In the present study, as the first step, we investigate the effect of inhomogeneity of ionospheric Hall conductance distribution. The background of this direction is the recently proposed concept of ionospheric control [Yoshikawa et al, 2008; 2013a, Nakamizo et al., SGEPSS, 2013] based on generalized theory for ionospheric polarization/Cowling channel formations [Yoshikawa et al, 2008; 2013b]
As for (B), normally either the Neumann or Dirichret conditions are selected for MHD variables (plasma density/pressure, velocity, deviation components of magnetic field from the intrinsic field). Other adjustments, representing particle precipitations, neutral wind friction, polar wind, and so on, are included. In the present study, we perform simulations with different pairs of boundary conditions for MHD variables.
In this presentation, we compare and discuss the obtained results.

Keywords: M-I Coupling, Ionospheric Polarization Field, Hall Conductance Inhomogeneity, Substorm, Global Magnetosphere MHD Simulation, Inner Boundary Conditions

Geomagnetic Phenomena near the AUTUMNX Magnetic Array in Québec, Canada

*Martin G Connors[1,2,3], Ian Schofield[1], Kyle Reiter[1], Christopher T Russell[5], Sebastien Guillon[4], Paul Prikryl[6,7], Kazuo Shiokawa[2], Mark Engebretson[8], Peter Chi[5], Jesper Gjerloev[9]

1. Athabasca University, 2. ISEE, Nagoya University, 3. Department of Physics and Astronomy, University of Calgary, 4. Hydro Quebec, 5. IGPP, UCLA, 6. University of New Brunswick, 7. Geomagnetic Laboratory, NRCan, 8. Augsburg College, 9. Applied Physics Laboratory, Johns Hopkins University

The AUTUMNX Magnetic Array's main chain has a closely-spaced set of UCLA THEMIS-class magnetometers along the east coast of Hudson Bay. Stations at Sept-Îles and Scheffervill, Québec, along with the THEMIS station at Kuujuaq and the NRCan Iqaluit observatory on Baffin Island make a looser second chain. This chain may be extended by a proposed new partner site in Fredericton, New Brunswick, and there are several other subauroral stations near the Hydro-Québec power grid. AUTUMNX magnetic data is freely available with one minute and 2 Hz cadence at http://autumn.athabascau.ca/autumnxquery.php?year=2017&mon=02&day=02 and pages easily accessed from there. It is also distributed widely, and in near-real time, to the THEMIS project, and quickly accessible through CDAWeb. More than one year of baselined one-minute cadence data (to the end of 2015) is now available through SuperMAG at http://supermag.jhuapl.edu/mag/. Since its establishment in late 2014, AUTUMNX has had a high rate of reliability and gathered nearly continuous data. For dates through mid-2016, however, potential users are urged to contact the PI about initial data quality issues at some sites. AUTUMNX is complemented by other arrays in eastern North America to now give good coverage in this region, which before 2014 had few magnetometers. AUTUMNX also improves magnetic data coverage near the footpoint of GOES East. It has magnetic conjugate points on land/ice in Antarctica, where the PRIMO project hopes to put new magnetometers.

The dense coverage of the Eastern Hudson Bay part of AUTUMNX allows magnetic inversion studies to be done well. Here we use techniques based on forward modelling to analyze cross meridian and regional currents. In addition to substorms, some of small total current, we find that steady convection is common. The currents in the March 17, 2015 storm attained 3 MA. A new finding relevant to space weather is that impulsive events are common. The Hydro-Québec utility measures harmonic distortion in the grid, and we find a close correlation with impulsive events. Our first detection of a pulse subsequently found to cause GIC in the Hydro-Québec network was on February 2, 2017 (link given above). In approximately 50 other cases, we have verified that GIC pulses initially detected in the grid had associated magnetic impulses. These are sometimes associated with substorms, but those which are not often show direct correlation with solar wind changes.

The AUTUMNX array has distinct advantages for ground magnetic studies in which high data rate, coverage of a large region, at least one closely spaced meridian chain, and conjugacy to geosyncronous satellites are important. We have also compared magnetic data with that from nearby GPS stations to show colocation of the auroral electrojets with scintillation during a storm. To these we currently add proximity to the major Hydro-Québec power grid servicing eastern North America for studies on space weather effects. There is further the potential for interhemispheric studies both on the conjugate magnetic footpoints in Antarctica at latitudes interesting for substorm studies, and along the meridian overlapping with Asia for day/night studies.

AUTUMNX was built with support from the GO Canada programme of the Canadian Space Agency, which now supports its operation.

Keywords: geomagnetism, magnetometer, data inversion, GIC, substorm, magnetic conjugacy

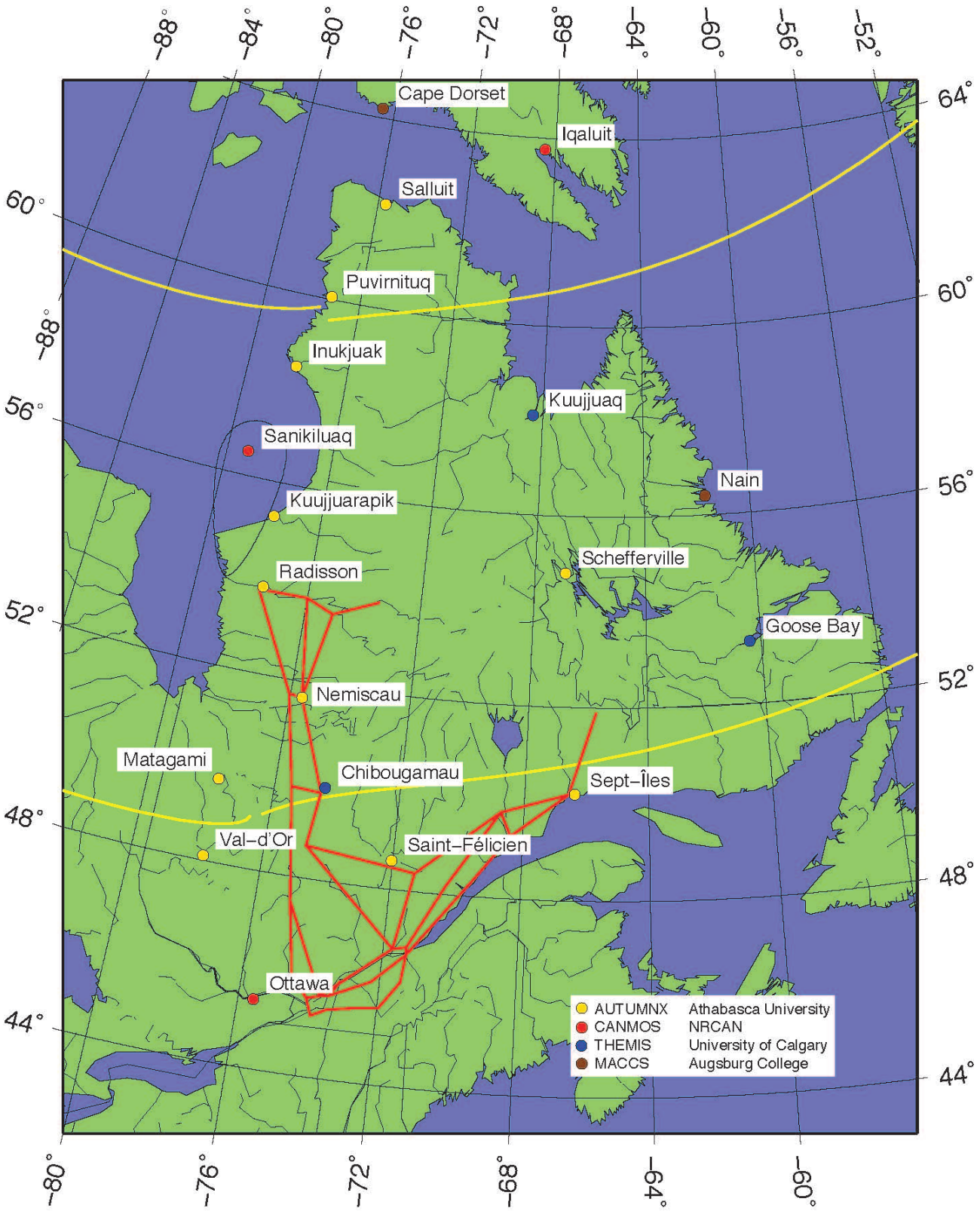

Application of Global Three-Dimensional Current Model for Dayside and Terminator Pi2 Pulsations

*Shun Imajo[1], Akimasa Yoshikawa[1,2], Teiji Uozumi[2], Shinichi Ohtani[3], Aoi Nakamizo[4]

1. Earth and Planetary Science, Kyushu University, 2. ICSWSE, Kyushu University, 3. APL, Johns Hopkins University, 4. AERI, NICT

We tested the magnetospheric-ionospheric current system for Pi2 magnetic pulsations on the dayside and near the terminator using a numerical model. We estimated the spatial distribution of the ground magnetic field produced by the three-dimensional magnetospheric-ionospheric current system for Pi2 consisting of field-aligned currents (FACs) localized in the nightside auroral region, the magnetospheric closure current flowing in the azimuthal direction, and horizontal ionospheric currents produced by the FACs in the electrostatic approximation. The calculated magnetic field reproduced the observational features reported by previous studies; (1) the sense of the H component is not changed over the wide local time sectors in low latitudes; (2) the amplitude of the H component on the dayside is enhanced at the equator; (3) D-component magnetic fields are reversed near the dawn and dusk terminators; (4) the meridian of the D-component phase reversal around the dusk terminator shifted more sunward than that around the dawn terminator; (5) the amplitude of the D component in the morning was larger than in the early evening. The separation of contributions to magnetic fields produced by each current part provides information on what contributes to these features. The phase reversals of the D component around dawn and dusk terminators are explained by a change in the contributing currents from the FACs on the nightside to the meridional ionospheric currents on the sunlit side of the terminator, and vice versa. The contribution of the ionospheric current on the dayside at middle-to-low latitudes is about 90%, suggesting that the spatial pattern of equivalent currents, which are magnetic field vectors rotated by 90 degrees, reflects that of ionosphere currents on the dayside. The different features between dawn and dusk regions can be attributed by the skewed dayside ionospheric current that has more intensive meridional currents in the morning than in the early evening. The model results indicated that the oscillation of the magnetospheric-ionospheric current system is a plausible explanation of Pi2 pulsations on dayside and near the terminator.

Keywords: Pi2 pulsation, magnetospheric-ionospheric current system, solar terminator, numerical model

Throat aurora and the important implications on solar-wind/magnetosphere coupling

*Han Desheng[1]

1. Polar Research Institute of China

Observational properties of throat aurora are investigated in detail by using 7-year continuous auroral observations obtained at Yellow River Station (magnetic latitude 76.24°N). From our inspection, throat aurora is often observed under the condition of stripy diffuse aurora contacting with the persistent discrete auroral oval, and the long-period throat aurora observations generally consist of intermittent subsequences of throat aurora brightening followed by poleward moving auroral form (PMAF) and throat aurora dimming. We also noticed that the orientation of throat aurora is aligned along the ionospheric convection flow and its local time distribution shows clear dependence on the interplanetary magnetic field (IMF) *By* component. These observational results indicate that factors inside the magnetosphere may play important role on occurrence of throat aurora. We thus suggest that throat aurora may present the ionospheric signature of redistribution of reconnection rate on the magnetopause by cold magnetospheric plasma flowing into the reconnection site. In addition, we also found that the occurrence rate of throat aurora clearly decreases with increase of the IMF cone angle (arccos(|*Bx*|/*B*)), which is very similar with the occurrence rate of high-speed jet (HSJ) observed in magnetosheath depending on the IMF cone angle. This is suggested as that the HSJs occurred outside the magnetosphere may also play important role for generation of throat aurora by triggering magnetopause reconnection or by direct impacting. Although further studies are needed to clarify how the throat auroras are generated in detail, the relevant observations about throat aurora have presented important implications on a variety open questions, such as, distribution and generation of cold plasma structures in the outer magnetosphere, magnetopause deformation, and possible relation between HSJ and reconnection.

Keywords: throat aurora, convection, ionospheric outflow, cold plasma, magnetic reconnection

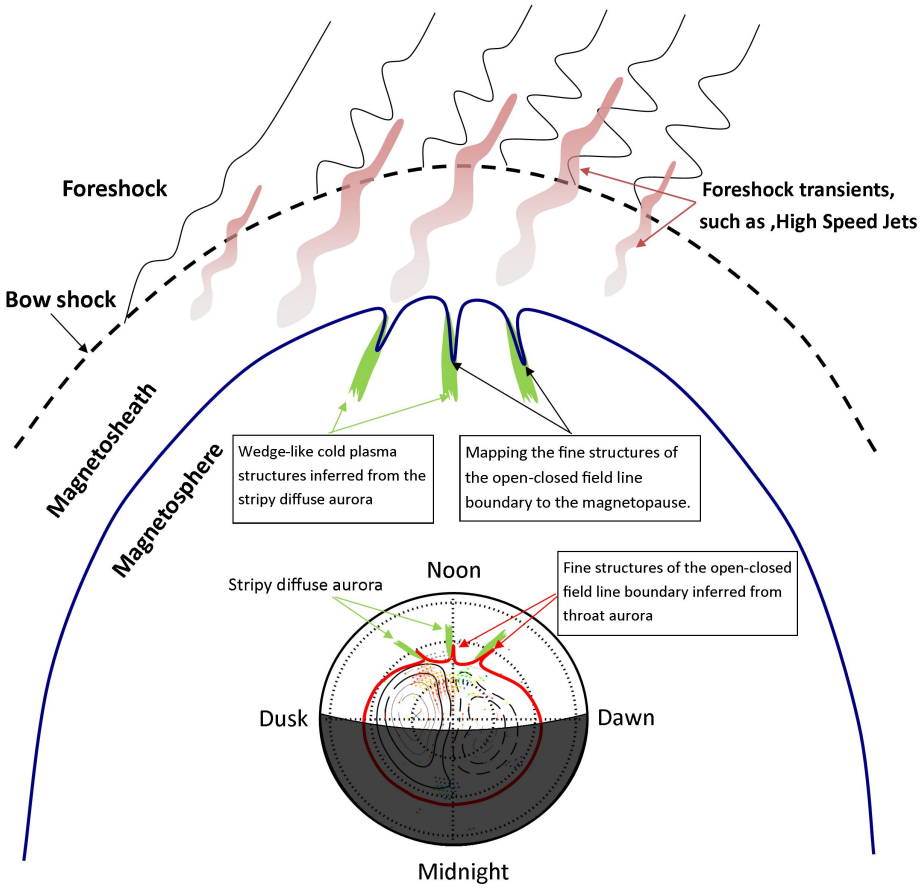

East-west band poleward moving long period (T~2-10 min) auroral pulsations

*Natsuo Sato[1,2], Akira S Yukimatu[1,2], Yoshimasa Tanaka[1,2], Tomoaki Hori,[3,4], Akira Kadokura[1,2]

1. National Institute of Polar Research, 2. SOKENDAI, 3. Institute for Space-Earth Environment Research, Nagoya University, 4. Department of Earth and Planetary Science, Graduate School of Science, The University of Tokyo

Using the ground-based all-sky imagers we examined the long period (T~ 2-10 min) east-west band type auroral pulsations which are completely different from well-known pulsating auroras with period of ~ 10 second. Fundamental characteristics of this type of auroral pulsations are as follows: 1) East-west band auroras extending more than 3000km in some cases, 2) Recurrently poleward moving auroral forms, 3) Recurrent periods are ~ 2-10 min, 4) Auroral intensity enhancement, not intensity modulation, 5) Occurrence region is just poleward side of common pulsating aurora, 6) Occurrence local time is post-midnight sector, 7) Aurora luminosity is rather high, sometimes comparable to discrete auroral arcs in the evening sector. We will examine the generation characteristics and mechanisms of this type of auroral pulsations using the multi-instrument ground-based observations and also the date simultaneously observed with instruments onboard spacecraft.

Keywords: aurora, east-west band aurora, auroral pulsation, pulsating aurora, magnetosphere-ionosphere coupling, polar region

Energetic electron precipitation and auroral morphology at the substorm recovery phase

*Shin-ichiro Oyama[1], Antti Kero[2], Craig J Rodger[3], Mark A Clilverd[4], Yoshizumi Miyoshi[1], Noora Partamies[5,6], Esa Turunen[2], Tero Raita[2], Pekka T Verronen[7], Shinji Saito[1]

1. Institute for Space-Earth Environmental Research, Nagoya University, 2. University of Oulu, 3. University of Otago, 4. British Antarctic Survey, 5. The University Centre in Svalbard, 6. Birkeland Centre for Space Science, 7. Finnish Meteorological Institute

It is well known that auroral patterns at the substorm recovery phase are characterized by diffuse or patch structures with intensity pulsation. According to satellite measurements and simulation studies, the precipitating electrons associated with these aurorae can reach or exceed energies of a few hundred keV through resonant wave-particle interactions in the magnetosphere. However, because of difficulty of simultaneous measurements, the dependency of energetic electron precipitation (EEP) on auroral morphological changes in the mesoscale has not been investigated to date. In order to study this dependency, we have analyzed data from the European Incoherent Scatter (EISCAT) radar, the Kilpisjärvi Atmospheric Imaging Receiver Array (KAIRA) riometer, collocated cameras, ground-based magnetometers, the Van Allen Probe satellites, Polar Operational Environmental Satellites (POES), and the Antarctic-Arctic Radiation-belt (Dynamic) Deposition-VLF Atmospheric Research Konsortium (AARDDVARK). Here we undertake a detailed examination of two case studies. The selected two events suggest that the highest energy of EEP on those days occurred with auroral patch formation from post-midnight to dawn, coinciding with the substorm onset at local midnight. Measurements of the EISCAT radar showed ionization as low as 65 km altitude, corresponding to EEP with energies of about 500 keV.

Keywords: aurora, ionosphere, EISCAT, KAIRA, energetic electron precipitation

A Comparison of Gamma and Lognormal Distributions for Characterizing Dst Variations of Long-lasting Geomagnetic Storms

*M. Chantale Damas[1], Jason Chou[1], Ying Dong[1]

1. Queensborough Community College of the City University of NY (CUNY)

In this study, the Disturbance Storm Time (Dst) profile of long-lasting storms are investigated. Dst variations for the entire duration of storms are approximated using both gamma and lognormal distributions. Profiles of fifty storms were evaluated so far and preliminary analysis showed that the Gamma distribution function may be a better fit overall than the lognormal distribution. Although both distributions tend to approximate the main phase of storms reasonably well, the gamma distribution function tend to approximate the recovery phase much better. Further analysis also shows that the gamma distribution function is also a much better fit than the lognormal distribution for storms caused by ICMEs as opposed to CIR storms. This may due CIR storms long duration recovery phases that can sometimes last days to weeks. This also applies to other storms such as High-Intensity, Long-Duration, Continuous AE Activity (HILDCAA) events with highly fluctuating magnetic fields. Of interest, energy dissipation is also modeled as a diffusion-like process where a 1-D diffusion profile would be equivalent to a Gamma distribution of k = 0.5. Profiles of evaluated storms show this diffusion-like profile suggesting the existence of a diffusion-like process in the energy dissipation in the ring current. More storms are being added to this study to further support our analysis and conclusion. Methods used and results will be discussed

Keywords: Dst, Geomagnetic Storms, Ring Current, ICMEs, CIRs, HILDCAA

Origin of the interplanetary magnetic field B_y-controlled field-aligned current systems on the dayside

*Masakazu Watanabe[1,2], Takashi Tanaka[1], Shigeru Fujita[3]

1. International Center for Space Weather Science and Education, Kyushu University, 2. Graduate School of Science, Kyushu University, 3. Meteorological College

It is well accepted that the field-aligned current systems (FACs) on the dayside are controlled by the dawn-dusk (B_y) component of the interplanetary magnetic field (IMF). We here describe the FAC systems for southward IMF. During IMF B_y-dominated periods, there appears a pair of FAC sheets in the midday sector. When IMF B_y is positive, in the Northern Hemisphere, the equatorward current flows into the ionosphere while the poleward current flows away from the ionosphere. The flow directions are opposite in the Southern Hemisphere. When IMF B_y is negative, the above-mentioned flow directions reverse. Although the morphology is well established, as for the understanding of the magnetospheric sources of those currents, there has been almost no progress in the past two decades. This is because what we can know from observations is very limited. To overcome the difficulty, we performed numerical magnetohydrodynamic simulations using the REPPU (Reproduce Plasma Universe) code recently developed by T. Tanaka. In the talk, we discuss the dynamo processes revealed by the numerical modeling.

Keywords: field-aligned current, magnetospheric dynamo, magnetohydrodynamics

The influence of IMF cone angle on invariant latitudes of polar region footprints of FACs in the magnetotail: Cluster observation

*Zhengwei Cheng[1], JianKui Shi[1], Jichun Zhang[2], Lynn M Kistler[2]

1. State Key Laboratory of Space Weather, NSSC/CAS, Beijing, 100190, China, 2. Space Science Center, University of New Hampshire, Durham, NH 03824, USA

Field-aligned currents (FACs) were detected by satellites in the 1960s for the first time [*Zmuda et al.*, 1966; *Cummings et al.*, 1967], and they have been observed at both low [*Iijima et al.*, 1978] and high [*Frank et al.*, 1981] altitudes in different regions in geospace. The large scale (from the magnetotail to the ionosphere) FACs are involved in many important physical processes, including field-aligned particle acceleration [*Morooka et al.*, 2004; *Shi et al.*, 2014], magnetic reconnection in the magnetotail [*Ma and Otto,* 2013], development of the substorm current wedge [*Hesse and Birn*, 1991], and auroral activity [*Elphic et al.*, 1998; *Xiong et al.*, 2014].
In solar wind-magnetosphere-ionosphere interactions, the large scale FACs play a crucial role in transferring the solar wind energy and momentum from interplanetary space to low altitude ionosphere. The solar wind and interplanetary magnetic field (IMF) affect the energy transfer process and the associated FACs directly. In the magnetosphere, the importance of the IMF cone angle is not controversial because it is closely concerned with many important physical phenomena. Some studies show that the IMF cone angle effects geomagnetic pulsations (Pc2-5 pulsations) [*Takahashi et al.*, 1984]. *Kavosi and Raeder* [2015] found that the occurrence rate of the Kelvin–Helmholtz waves (KHWs) in the magnetopause increases with the IMF cone angle. Also, the IMF cone angle can control the efficiency of reconnection at the subsolar point [*Scurry et al.*, 1994]. Some authors have suggested that the IMF cone angle can even influence the magnetopause location [*Dušík et al.*, 2010]. In the magnetotail, both IMF cone angle and clock angle are the important factors and have great influences on the FACs. *Cheng et al.* [2013] found the FAC occurrence in the magnetotail increases monotonically with the IMF cone angle. The FAC is a large scale phenomenon in the magnetosphere-ionosphere system. The FACs in the Plasma Sheet Boundary Layers (PSBLs) connected with those in the polar region through the magnetic field lines [*Wild et al.*, 2004] and they are important for the energy flows in the solar wind-magnetosphere-ionosphere system. How the solar wind affects the large scale FACs from the magnetotail to the polar region is still an open question. And no study on the relationship between the IMF cone angle and the invariant latitudes of the FACs in the PSBLs in the magnetotail has been done. This study is focused on the influence of the IMF cone angle on the projection locations of the observed FACs by Cluster in the northern PSBL in the magnetotail. We performed a statistic study of 542 FAC cases observed by the four Cluster spacecraft in the northern hemisphere. The results show that the large FAC (>10 nA/m^2) cases occur at the low ILATs (<71 º) and mainly occur when the IMF cone angle θ >60º, which implies the footprints of the large FACs mainly expand equatorward with large IMF cone angle. The equatorward (poleward) boundary of the FAC footprints decreases (increases) with the IMF cone angle. The equatorward boundary is more responsive to the IMF cone angle. This is the first time a correlation between FAC projected location and IMF cone angle has been determined.

Keywords: FAC in magnetotail, Footprints in polar region, IMF cone angle

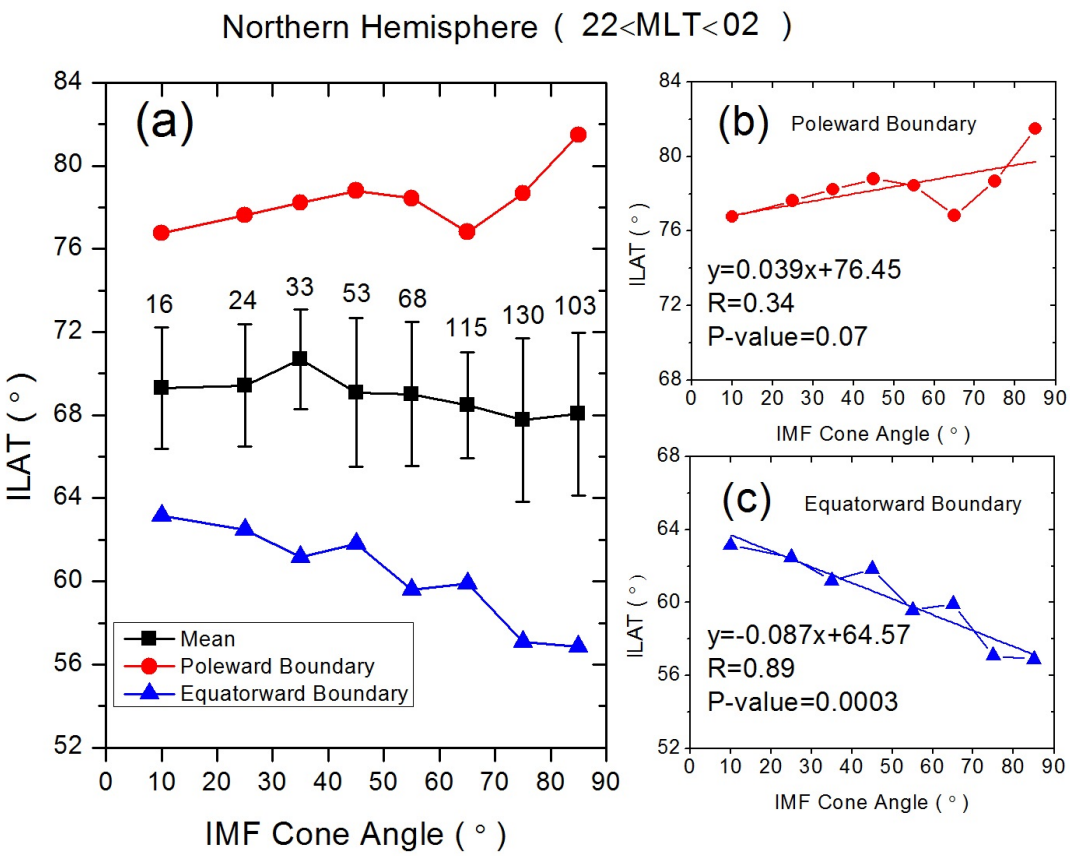

Simulation study of the driving mechanism of the magnetosphere-ionosphere coupling convection

*Shigeru Fujita[1], Takashi Tanaka[2], Masakazu Watanabe[3]

1. Meteorological College, Japan Meteorological Agency, 2. REPPU code institute, 3. Graduate School of Sciences, Kyushu University

The Region 1 field-aligned current (R1FAC) controls the magnetosphere-ionosphere coupling convection. The global MHD simulation reveals that the dynamo of the R1FRC appears in the cusp-mantle region [Tanaka, 1995]. So, in order to elucidate the driving mechanism of the convection, we investigate the link between the solar wind energy and the dynamo of the R1FAC by analyzing the numerical results of the global MHD simulation in the southward IMF condition. This study presents an alternative model of the magnetosphere convection proposed by Dungey (1961). First, the flow motional energy in the solar wind is converted to the thermal energy in the bow shock. This thermal energy is transported to the magnetopause reconnection region. Second, plasma acceleration due to the reconnection in the dayside magnetic field configuration of the null-separator structure does not directly drive the dynamo of the R1FAC. The plasmas in the magnetosheath also contribute to the plasma acceleration. Third, the accelerated plasmas are decelerated when they are transported to the high-latitude magnetosheath next to the cusp. This deceleration invokes the local dynamo. This local dynamo does not drive the R1FAC. This result indicates that the mechanical energy from the solar wind does not directly contribute to driving the R1FAC dynamo. Plasma acceleration in the reconnection region and formation of the local dynamo can be called as the local Dungey process. Fourth, the magnetic energy produced in the local dynamo is transported to and deposited as the thermal energy in the cusp entry region. This mechanism is called as the cusp bridge. Fifth, the thermal energy in the boundary region is accelerated along the field line into the cusp due to the field-aligned pressure gradient. Sixth, the field-aligned accelerated flow is converted to the perpendicular flow in the cusp due to the centrifugal force caused by the field-aligned flow along the bending field line in the cusp. The perpendicular flow goes to the cusp-mantle region. Last, the slow mode expansion mechanism invokes the dynamo of the R1FAC in the cusp-mantle region.

In the talk, we will present how the solar wind condition control the energy transport and conversion from the solar wind to the dynamo region of the R1FAC.

Keywords: magnetospheric convection, MHD simulation , energy conversion

A statistical study of the near-Earth magnetotail evolution duing substorms and pseudosubstorms with themis data

*Kento Fukui[1], Shinobu Machida[1], Yukinaga Miyashita[1], Akimasa Ieda[1], Yoshizumi Miyoshi[1], Angelopoulos Vassilis[2]

1. Institute for Space-Earth Environmental Research. Nagoya university, 2. University of California, Los Angeles

Substorms and pseudosubstorms (pseudobreakups) are very similar phenomena. In terms of auroral morphology, pseudosubstorms are generally more localized and more short-lived, compared with substorms, and are not accompanied by poleward expansion. We examined auroral development for events from November 2007 through April 2010, using data from THEMIS all-sky imagers. We defined events accompanied and not accompanied by poleward expansion as substorms and pseudosubstorms, respectively. To understand the cause of auroral development, we investigated temporal and spatial development of the near-Earth magnetotail during substorms and pseudosubstorms, based on superposed epoch analysis of THEMIS data. We find that Vx begins to increase at -9.5 >X(GSM)>-11.5 Re around onset for both substorms and pseudosubstorms. This seems to be due to earthward flows caused by magnetic reconnection. Bz also increase around onset at -9.5 >X>-11.5 Re both substorms and pseudosubstorms. The amount and rate of Bz change are larger for substorms than for pseudosubstorms. In the earthward (-7.5 >X>-9.5 Re) and tailward (-11.5 >X>-15.5 Re) regions, Bz increases substantially for substorms, whereas it does not increase very much for pseudosubstorms. These results indicate that dipolarization is weaker for pseudosubstorms than for substorms, and the dipolarization region does not spread extensively for pseudosubstorms. In addition, Brms begins to increase at -6.5>X>-11.5 Re around onset both substorms and pseudosubstorms. The amount of Brms change is larger for substorms than for pseudosubstorms, indicating that waves are strongly induced for substorms. These waves are considered to be caused by instability, and the instability takes place in more for substorms and not in pseudosubstorms. We, therefore, suggest that the occurrence of the instability develops tailward to form the current disruption region and causes auroral poleward expansion. Meanwhile, the plasma and magnetic pressures increase at -6.5 >X>-7.5 Re after onset in association with dipolarization, particularly for substorms. The total pressure (the sum of the plasma and magnetic pressures) prior to the onset is larger in that region for substorms than for pseudosubstorms. At -7.5 >X>-9.5 Re the total pressure hardly differ between substorms and pseudosubstorms. Thus we conclude that the spatial gradient of the total pressure is a key that determines whether the current disruption take place, that is, whether initial activation develops into a substorm or into a subsiding pseudosubstorm.

Keywords: substorm

Simultaneous satellite-ground observations of shock triggered substorm expansion

*Jianjun Liu[1], Hongqiao Hu[1], Desheng Han[1]

1. Polar Research Institute of China

Interplanetary (IP) shock encountering the terrestrial magnetosphere can greatly disturb the Earth’s electromagnetic environment and hence intensify the global current system. Here, we examine a distinguishable compression associated auroral event caused by an IP shock sudden impingement to the magnetosphere. We utilize IMAGE satellite auroral imager to obtain the broad global-scale auroral oval over Southern Hemisphere. It is fortunate that part of the nightside poleward branch of the oval was monitored by simultaneous ground-based high temporal-spatial resolution all-sky camera at Antarctic Zhongshan Station (-74.5º magnetic latitude). Satellite imager recorded aurora sudden brightening in pre-midnight just after the IP shock arrival to the magnetosphere. Intensified large-scale aurora experienced interesting azimuthal movement. The poleward and equatorward boundary of the nightside aurora oval featured dramatically enhanced auroral emission with broaden oval width, which presented obvious so-called double auroral oval structure. It is shown that ground-based optical auroral sequential images present prominent westward surge in the poleward branch of the nightside auroral oval, and the westward surge structure shows typical poleward boundary intensifications with periodical signature. This auroral periodical enhancement corresponds well to the geomagnetic variation recorded by the fluxgate magnetometer at Zhongshan station. It is suggested that for substorm triggered by sudden enhanced solar wind dynamic pressure in the precondition of southward IMF, the triggering could occur quite instant after increased dynamic pressure hits on the magnetopause.

Keywords: Interplanetary shock, double auroral oval, substorm expansion

Temporary shrinkage of the near-equatorial tail after the substorm expansion onset

*Hideaki Kawano[1,2], Kazuma Shirotani[1]

1. Department of Earth and Planetary Sciences, Kyushu University, 2. International Center for Space Weather Science and Education, Kyushu University

Kawano et al. (2000) presented a case of three recurring substorms, in which the GEOTAIL spacecraft, located in the magnetotail near the equatorial part of the tail magnetopause, temporarily exited the tail and then returned to the tail after the expansion onset for all of the three substorms. The position of GEOTAIL was near (-42, -22, 0) [Re].

They suggested that this phenomenon was caused by the temporary shrinkage of the mid-tail equatorial magnetosphere after the expansion onset, and that the shrinkage was likely to have been caused by the near-Earth neutral line (NENL). That is, as the NENL ejected plasma in the radial direction away from the NENL, it drew in plasma along the line including the NENL toward the NENL, and thus the magnetopause near that line moved inward.

In this paper, we have constructed a database of this kind of events observed by GEOTAIL between Oct. 5, 1993 and Dec. 31, 2002, and examined if the above-stated interpretation is valid. In more detail, we have first identified magnetopause crossings of GEOTAIL based on its observation of the plasma density, temperature, and tailward velocity. We have then selected crossing pairs, i.e., entry-exit pairs and exit-entry pairs, by using the following two criteria: (1) an entry and its paired exit were separated in time by less than three hours; (2) during the four hours consisting of two hours preceding the pair-event start time and two hours following the event end time, GEOTAIL was in the same region (i.e., inside or outside the magnetosphere). We have also identified, as an independent procedure, substorm expansion onsets by using the AL index, and compiled them into another database. Then, for each of the above-identified crossing pairs, we have selected a corresponding substorm onset if the former started less than three hours before or after the latter.

After the above-stated event-selection procedure, we have first compared the starting times of the exit-entry pairs and the substorm expansion onset times. As a result, we have found that the majority of them started after (i.e., not before) the substorm expansion onset, consistent with the temporary-shrinkage interpretation by Kawano et al.

We have also compared the ending times of the entry-exit pairs (which were not studied by Kawano et al.) and the substorm expansion onset times. As a result, we have found that the majority of them ended near the substorm expansion onset time.

More details, including the position dependence of the event occurrence frequency and the time separation between the substorm onset and the event, will be presented at the meeting.

Toward the unified model of substorm

*Shinobu Machida[1], Kento Fukui[1], Yukinaga Miyashita[1], Akimasa Ieda[1]

1. Institute for Space-Earth Environmental Research, Nagoya University

Numerous models of substorms have been proposed so far, and they are roughly divided into two categories, i.e., an outside-in category that is represented by the NENL model and an inside-out category that is represented by the ballooning instability model. Controversies have been raised for many years over the validity of those models. However, in recent years we have obtained extremely important clues to solve this long-standing issue by separately analyzing THEMIS probe data for substorms and pseudo-substorms. [Fukui et al., 2017]
The key is the plasma pressure in the equatorial region, and in the case of the substorm, it was about 1.4 and 1.2 times larger in the region of X ~ -7 and -8 Re than in the case of the pseudo-substorm. However, no difference was found beyond X~ -10 Re. Therefore, the spatial gradient of the plasma pressure in the region of X ~ -7.5 Re must be a necessary condition for substorm.
An occurrence of abrupt earthward flows originated from the catapult current sheet relaxation and subsequent magnetic reconnection at the NENL just prior to the onset is a common signature for both substorm and pseudo-substorm. Those flows must initiate some instability, possibly the ballooning instability in the earthward side of the flow front.
Substorms do not occur only with the magnetic reconnection. If there is enough plasma pressure gradient, the system can develop into a substorm. Otherwise, it will end up with a pseudo-substorm. We emphasize that both NENL model and the ballooning instability model are partially correct but incomplete, and a true model of substorm can be constructed by combining at least these two.

Keywords: substorm, pseudo-substorm, magnetic reconnection, ballooning instability

Evolution process of the theta aurora inferred from global MHD simulations

*Kyoko Mimura[1], Takahiro Obara[2], Shigeru Fujita[3]

1. Faculty of Science,Tohoku University, 2. Planetary Plasma and Atmospheric Research Center, Tohoku University, 3. Meteorological College, Japan Meteorological Agency

The theta aurora sometime appears in the polar cap region when IMF Bz keeps northward.
There are many previous studies, but no unified theory to explain what happens in the ionosphere and magnetosphere during the theta aurora events.

We made MHD simulation by changing IMF By polarity from negative (-4.3nT) to positive (4.3nT) under the northward condition (Bz=4.3nT). Simulation results show there are three stages of the theta aurora evolution. First stage is characterized by the rapid change (within about several minutes) of the anti-clockwise convection to the clockwise one viewed from the north pole in the cusp region of the northern hemisphere. At the same time, upward Region 0 FACs in the post-noon region is exchanged with downward Region 1 FACs in the pre-noon region. Associated with the switch of the FAC polarity in the dayside ionosphere, the dynamo location is also shifted from the post-noon region to the pre-noon region in the dayside magnetosphere. Second stage is characterized by the detachment of high pressure region from the cleft. The detached region move to the high latitude lobe region in the night side and gradually becomes short. This stage lasta about 30 minutes. The high pressure region correspond to the moving front of the changing convection flow. A pair of upward and downward FACs in the ionosphere appears in association with the moving high-pressure region in the magnetosphere. The dynamo appears in the high-pressure region in the magnetosphere as noted below. The closed field line region breaking into the polar cap region associates the pair of the FACs in the ionosphere. We notice that the high-pressure region in the magnetosphere corresponds to the closed field line region. Third stage is given by the extension of the high pressure region to the dayside aurora region. Disturbances in the magnetosphere and in the ionosphere caused by the By change gradually disappear. The FACs become weak, but the closed field line region still beaks into the polar cap. The high-pressure region in the magnetosphere is located in the closed field line region in this stage, too.

It is strongly expected that high pressure region connect to the dynamo region($E \cdot J<0$), we have examined field aligned current signature in high pressure region for three stages. The results demonstrate that pressure region connect to the dynamo region($E \cdot J<0$),consistent with Watanabe et al.(2014). We will report a possible mechanism to generate the dynamo region and its relation to the theta aurora formation in the presentation. It is the final goal of this study to elucidate the state transition mechanism of the magnetosphere-ionosphere compound system caused by the IMF By change.

Study of the plasma sheet electron inner boundary during the magnetic storm

*Kento Ohki[1], Atsushi Kumamoto[1], Yuto Katoh[1]

1. Department of Geophysics, Graduate School of Science, Tohoku University

The locations of the inner boundary of the plasma sheet electrons during magnetic storm have been analyzed by using the dataset from Time History of Events and Macroscale Interactions during Substorms (THEMIS) satellites.
The dependence of the location of the inner boundary of the plasma sheet electrons on geomagnetic indices such as Kp and AE was investigated in several previous studies [Korth et al., 1999; Jiang et al., 2011]. In addition, several empirical convection electric field model such as Volland-Stern model [Volland, 1973; Stern, 1975], McIlwain's E5D model [McIlwain, 1986], Weimer model [Weimer, 1996], and Matsui Model [Matsui et al., 2013] have been proposed based on the statistical analyses. So, we can trace the expected drift path of the plasma sheet particles in these electric filed models, and compare them with observed locations of the plasma sheet inner boundary.
In this study, we investigated the locations of the inner boundary of the plasma sheet electrons during the magnetic storms by using the electron flux data of 9 keV obtained by Electrostatic Analyzer (ESA) onboard the THEMIS satellites. We determined open/close boundary of the drift paths of plasma sheet electrons in Volland-Stern electric field during the recovery phase of the magnetic storm by performing the test particle simulation, and compared it with the position of the inner edges of the plasma sheet 9-keV electron measured by THEMIS ESA in the same period, because it is a simple macroscopic electric field model depending on slow variation of Kp, and good for the reference to find out the contributions of storm-time electric fields probably with rapid changes and microscopic structures.
We performed the statistical analysis of the positions of the inner edge identified in the recovery phase in the case that differences between the observed plasma sheet electron inner boundary and the open/close boundary of the energetic electron drift path calculated with Volland-Stern convection electric field model [Volland et al., 1973] are less than 0.5 RE. The agreement in these events suggests that the storm-time electric field does not exist around the calculated drift paths. However, as for three of twenty-two events, the calculated drift paths overlap the intense storm-time electric field reported by Nishimura et al. [2008]. In the event on December 20, 2015 around 20:00 MLT (Case-1), the geocentric distance of open/close boundary of the drift path of plasma sheet electrons, Rmodel, is 3.97, and that of the inner edge of the plasma sheet electrons in the magnetic equatorial plane, Robs, is 3.93. We calculated the electric field without the corotation electric field at the plasma sheet electron inner boundary found using Volland-Stern model, and compared it with the storm-time electric field reported by Nishimura et al. [2008]. Ex in the GSM coordinate calculated with Volland-Stern model (Exvs) is 0.23 mV/m while that reported by Nishimura et al. [2008] (Exni) is about -4.00 mV/m. If such large electric field exists on the drift path, the open/close boundary based on Volland-Stern electric field deviates from that of the inner edge of the plasma sheet electrons. From the analysis of another event on October 1, 2012 around midnight (Case-2), Rmodel is 3.50, Robs is 3.18, Exvs is 0.06 mV/m and Exni is about -3.00 mV/m. And as for a event obtained on July 9, 2012 around 20:00 MLT (Case-3), Rmodel is 6.18, Robs is 6.00, Exvs is 0.14 mV/m and Exni is about -1.00 mV/m. In this event, the calculated drift path doesn't overlap the intense storm-time electric field reported by Nishimura et al. [2008]. From the analysis of another event on February 2, 2015 around 19:00 MLT (Case-4), Rmodel is 7.01, Robs is 7.39, Exvs is 0.07 mV/m and Exni is about -1.00 mV/m.
We focus on Dst index in order to check the above difference. From the analysis of Case-1, Dst index is

the smallest in all event and is -155 nT. From the analysis of Case-2, Dst index is the second smallest, and -102 nT. On the other hand, in the event of Case-3 and Case-4, Dst index is -66 and -46 nT. It is considered that plasma sheet ions and electrons distributed in a wide MLT region from the dusk to postmidnight are gathered into the dusk to premidnight sector in the region of enhanced electric field due to the strong ExB drift [Nishimura et al., 2008]. Although the storm-time electric field reported by Nishimura et al. [2008] is the average electric field distributin, from the result obtained on Case-1 - 4, it is considered that the actual storm-time electric field exists more inside during high activities, over 100 nT.

Keywords: magnetic storm, convection electric field, ring current

Local time and seasonal variations of the amplitude of the main impulse (MI) of geomagnetic sudden commencements in the low-latitude and equatorial regions

*Atsuki Shinbori[1], Takashi Kikuchi[1], Tohru Araki[2], Akihiro Ikeda[4], Teiji Uozumi[5], Hisashi Utada[6], Commodore Romeo Isidre Ho[7], Tsutomu Nagatsuma[3], Akimasa Yoshikawa[5]

1. Institute for Space-Earth Environment Research (ISEE), Nagoya University, 2. Kyoto University, 3. National Institute of Information and Communications Technology, 4. National Institute of Technology, Kagoshima College, 5. International Center for Space Weather Science and Education, Kyushu University, 6. Earthquake Research Institute, The University of Tokyo, 7. Hydrography Dept. National Mapping and Resource Information Authority

Local time and seasonal variations of the amplitude of the main impulse (MI) of geomagnetic sudden commencements (SCs) in the equatorial and low-latitude regions (geomagnetic latitude (GMLAT) range: 0 –30 degrees) has been investigated using high time resolution geomagnetic field data for the period 1996 –2009. These geomagnetic field data are provided by the Circum-Pan-Pacific-Magnetometer-Network (CPMN) [Yumoto and the CPMN Group, 2001] and National Institute of Information and Communications Technology (NICT) Space Weather Monitoring (NSWM) [Kikuchi et al., 2008]. In order to identify SC events from January 1996 to 2009, we used the SYM-H index with 1-minute time resolution archived on the web site of World Data Center for Geomagnetism, Kyoto University. In this study, total 6992 SC events were found as a sudden increase of the SYM-H index by more than 5 nT within 10 minutes 1during this period, corresponding to the solar wind dynamic pressure enhancement. The solar wind data are archived on the CDAWeb site. As a result, the local time dependence of the SC amplitude in the low-latitude region (10^{o} < GMLAT < 30^{o}) showed the semi-diurnal variation with two maxima around 10 –14 h (LT) and 22 –1 h (LT) and the two minima around 6 –9 h (LT) and 16 –19 h (LT), respectively. The peak value of the nighttime SC amplitude tended to be equal to or more than that of the daytime amplitude. The minimum value of the SC amplitude in the morning (4 –10 h, LT) tended to be smaller than in the afternoon. This morning-afternoon asymmetry in the SC amplitude is due to a magnetic effect of the two-cell ionospheric currents driven by the MI electric field. The size of the local time variation of the SC amplitude in the low-latitude regions becomes largest in the summer (May –July). During this period, the nighttime SC amplitude tended to be enhanced significantly and was larger than the daytime one. Moreover, the daytime (10 –14 h, LT) SC amplitude at OKI was enhanced significantly near the equinoxes (March and October). The seasonal variation of the SC amplitude at OKI during 10 –14 h (LT) showed a significant decrease during May –October. This depression cannot be explained only by the seasonal variation of the ionospheric conductivity. The local time variation of the SC amplitude in the equatorial region (GMLAT < 10^{o}) clearly showed the equatorial enhancement of the SC amplitude in the daytime (8 –17 h, LT). This enhancement is due to a magnetic effect of the eastward equatorial electrojet driven by a dawn-to-dusk electric field generated during the MI phase of SC. The nighttime enhancement of the SC amplitude as seen in the low-latitude region appeared also in the equatorial region (5.0^{o} < dip latitude < 20.0^{o}). This result suggests that a magnetic effect caused by a pair of FACs generated during the MI phase of SC extended near the equatorial region. The seasonal variation of the equatorial enhancement of the SC amplitude showed a significant depression by 3 –10 % in the summer (May –July), compared with that in the winter (November –January) in the northern hemisphere. The summer reduction of the SC amplitude can be seen at the GAM and MUT stations located near the dip equator. Moreover, the SC amplitude in the afternoon –evening (14 –21 h, LT) tend to decrease by 10 –30 % during March –September. This summer depression of the SC amplitude appears also at the dip equatorial stations (YAP and PON). From a comparison of the ionospheric conductivity and SC amplitude, it was shown that the decrease of the

equatorial enhancement in the morning –evening (8 –21 h, LT) cannot be explained only by the seasonal variation of the ionospheric conductivity. Therefore, the equatorial SC-MI reduction suggests a weakness of a dawn-to-dusk ionospheric electric field during the summer in the northern hemisphere.

Keywords: Geomagnetic sudden commencement, Seasonal variation, Local time variation, Ionospheric conductivity, Equatorial region, Ionospheric electric field

Athabasca University Geophysical and GeoSpace Observatories (AUGO and AUGSO)

*Martin G Connors[1], Ian Schofield[1], Kyle Reiter[1], Kazuo Shiokawa[2], Yuichi Otsuka[2], Mitsunori Ozaki[3], Yoshizumi Miyoshi[2], Ryuho Kataoka[4], Yoshimasa Tanaka[4], Kaori Sakaguchi[12], Reiko Nomura[13], Claudia Martinez-Calderon[5], Jun Chae-Woo[5], Kunihiro Keika[14], Akimasa Ieda[2], Trond Trondsen[6], Devin Wyatt[6], Craig Unick[7], Eric Donovan[7], Brian Jackel[7], Christopher Cully[7], Christopher T Russell[8], Noora Partemies[9], Mikko Syrjaesuo[9], Peter Dalin[10], Mark Zalcik[15], Anthony Tekatch[11], Doug Welch[11]

1. Athabasca University, 2. ISEE, Nagoya University, 3. Kanazawa University, 4. National Institute for Polar Research, 5. Department of Meteorology and Oceanography, UCLA, 6. Keo Scientific Limited, 7. Department of Physics and Astronomy, University of Calgary, 8. IGPP, UCLA, 9. The University Center in Svalbard, 10. Swedish Institute of Space Physics, 11. Unihedron Corporation, 12. National Institute of Information and Communications Technology, 13. ISAS, JAXA, 14. Department of Earth and Planetary Science, University of Tokyo, 15. NLC Can-Am Network

Athabasca University has operated geophysical instruments at AUGO (113º49’ 42” W,54º49’ 42” N) since 1998, and now (since 2012) most are located at AUGSO (113º38’ 40” W,54º36’ 10” N) in a very dark rural location. The geomagnetic latitude of about 61º, less than that of most comprehensive observatories, has led to insight into subauroral and transition region processes. The new AUGSO location has residential facilities capable of hosting up to 9 researchers for campaign style work or installation of equipment. An important feature is fiber optic internet access to both sites, allowing remote operation of instruments. Although most instruments have dedicated, restricted access, sky conditions may be verified, or live auroras may be viewed if they are present, when it is dark, at http://autumn.athabascau.ca/auroracamhd.htm . A magnetometer of the AUTUMN network has operated at the site since 1998, however should not be confused with the nearby NRCan observatory, Meanook. Sample data for the AUTUMN network during the St. Patrick’s Day Storm of 2015 may be found at http://autumn.athabascau.ca/autumnquery.php?year=2015&mon=03&day=17 . Navigation to other pages is easy from there. The AUTUMN sites do not all have the same type of magnetometer, but most take measurements every second, or at 2 Hz, and the data are publicly available and contributed to THEMIS and via there to CDAWeb.

Since 2003, imaging has been done from the Athabasca location. A NASCAM All-Sky Intensified imager was operated from 2004 to 2012, when it was superseded by an EMCCD-based multispectral imager manufactured by Keo Scientific Ltd., at the new, darker site. THEMIS allsky monochrome imagers were tested at Athabasca, and one currently operates there. In 2005, an OMTI multispectral imager was installed along with an H-beta spectrometer. A particularly fruitful field has been that of proton auroras, for which the subauroral location and very dark skies are well suited. Search coil magnetometer detection of Pc1 pulsations coincident with detached proton auroras showed the importance of EMIC waves in causing proton precipitation. More recent coordinated investigations have involved faster imaging so that pulsations in the proton aurora could be detected, as well as VLF emissions coincident with proton auroras and compression events. A riometer was recently installed. Instrument development has also been fostered by AUGSO, most notably the FESO meridian imager which is photomultiplier based with advanced background removal, taking H-beta detection into a new realm of sensitivity and temporal sampling. The combined comprehensive instrumentation is expected to soon be coordinated with in situ measurements by the ERG/Arase satellite, and some preliminary studies involving Van Allen probes have been done.

We continue to operate two sites, with the original one used mainly for instrument testing and support of

a telescope and non-auroral guest instruments. Some specialized studies benefit from having two sites, and we have been very successful in stereo imaging of noctilucent clouds (NLC). Rapid motion of auroral forms has meant less success in stereo studies, but there is great potential.
External instrument development has involved Canadian commercial companies Keo Scientific and Unihedron, both taking advantage of the auroral zone location for optical detection. We are extending our magnetometry and electronics expertise into other domains as well, with most testing done at AUGO.
Both AUGO and AUGSO were funded by the Canada Foundation for Innovation, which also makes a significant contribution to operating costs. The CANARIE computing consortium funded the innovative concept of connection to high speed fiber optic internet at the rural AUGSO site.

Keywords: auroral imaging, proton aurora, observatories, geomagnetism, noctilucent clouds

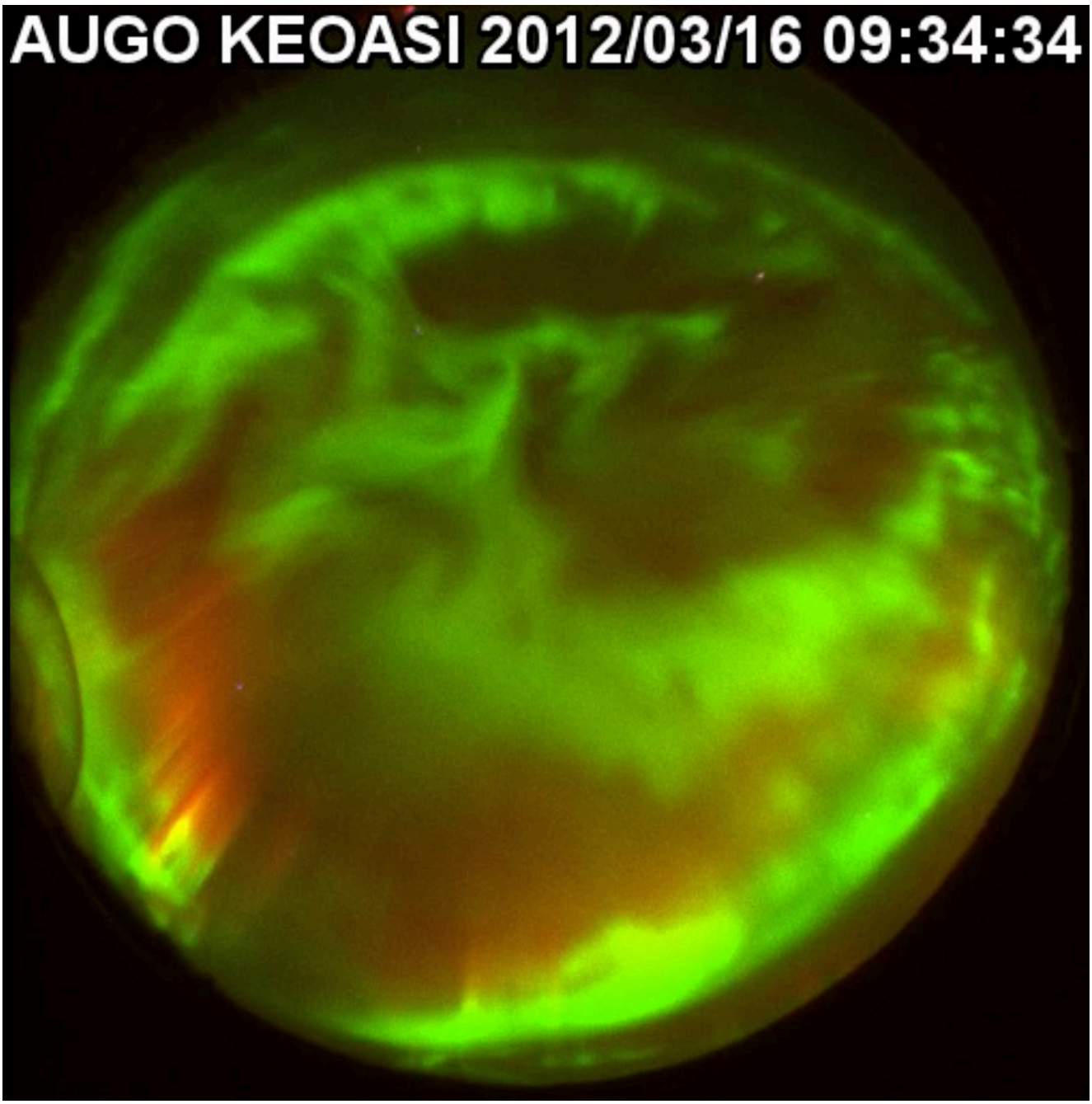

Ionspheric Conductivity Dependence of the Subauroral Polarization Streams Observed by the SuperDARN Hokkaido East HF Radar

*Yuting Zhang[1], Nozomu Nishitani[1], Tomoaki Hori[1]

1. Nagoya University

We investigate the characteristics of the subauroral polarization stream (SAPS), with a main focus on the solar zenith angle(SZA) dependence using the Super Dual Auroral Radar Network (SuperDARN) Hokkaido East radar and NOAA POES spacecraft data. In this study, we checked over 2830 days from 2008/1/10 to 2015/12/31 and found 29 SAPS events where the line-of-sight velocity is larger than 150m/s, magnetic local time is 13 to 19 hours and the flow regions are identified to be equatorward of the auroral precipitation region. For each event we examined the SZA using the geographic latitude, longitude and the UT span of SAPS. We identified the lowest possible SZA and lowest illuminated ionospheric altitude for SAPS to be generated, which have not been discussed in detail before. As a result of the statistical analysis, it is found that the SAPS tends to appear when the SZA is larger than 100 degrees, and that the lowest illuminated ionospheric altitude should be higher than about 100km for SAPS to appear. The minimal threshold of the illuminated ionospheric altitude is near the altitude of the peak of Pedersen conductivity. This result suggests that the Pedersen conductivity plays an important role for the generation of SAPS, which is consistent with the previous studies. Results of detailed discussion will be presented.

Keywords: solar zenith angle, magnetosphere-ionosphere coupling, Pedersen conductivity, sub-auroral polarization stream, SuperDARN Hokkaido East radar

Statistical analysis of ionospheric electric field oscillation associated with Sudden Commencement seen by the SuperDARN radars in the northern hemisphere

*Iida Kouhei[1], Nozomu Nishitani[1], Tomoaki Hori[2]

1. Institute for Space-Earth Environmental Research, Nagoya University, 2. Tokyo University

Sudden Commencement (SC) is observed mainly as a sudden increase of the H-component of geomagnetic field at low latitudes. Past studies showed that it is caused by a sudden compression of the magnetosphere associated with rapid increases of the solar wind dynamic pressure. At middle and high latitudes, SCs cause perturbations associated with twin vortex type ionospheric currents. It was reported that the disturbance of the ionospheric current and the electric field associated with SC consists typically of the Preliminary Impulse (PI) and the Main Impulse (MI). Previous studies reported that some of SC-associated electric field disturbances observed by SuperDARN radars show only the two successive pulses of PI and MI, while some others are accompanied by damped oscillations of the ionospheric electric field lasting for about several tens of minutes to an hour with periods of several minutes. The reason why both types of SC-associated disturbances can occur, however, have not yet been understood well. We examine the cause of the difference between the two kinds of SC events, using SuperDARN radars in the northern hemisphere covering ~40 to 90 degree geomagnetic latitudes. For the analyzed period from January 2011 to December 2015, 244 SC events were identified and 61 events out of them were accompanied by the ionospheric electric field oscillations immediately following MIs, as observed by at least one SuperDARN radar. We contrast 183 events (only PI and MI) with 61 events (oscillation following MIs) and find that the average of magnitude of dynamic pressure change does not seem to be the cause of the difference between two types of disturbance associated with SC events. On the other hand, a detailed analysis on the electric field oscillations shows that some of them exhibit phase differences in latitude and longitude, while the others not. These observations indicate that the ionospheric electric field oscillations sometimes show propagation characteristics. We examine frequencies of the electric field oscillations. We also discuss the magnetic local time (MLT) dependence of the ionospheric electric field oscillations as well as its dependence on spatial displacement of the magnetopause associated with SC.

Keywords: SuperDARN, Sudden Commencement, ionospheric electric field oscillation

Global mapping of ionospheric plasma velocity distributions using spherical elementary current systems based on SuperDARN data

*Shin'ya Nakano[1], Tomoaki Hori[2], Kanako Seki[2], Nozomu Nishitani[3]

1. The Institute of Statistical Mathematics, 2. Graduate School of Science, the University of Tokyo, 3. Institute of Space-Earth Environmental Research, Nagoya University

We have developed a method for estimating the global distribution of ionospheric plasma velocity from the SuperDARN data. The SuperDARN observations have a wide spatial coverage. However, it is difficult to obtain a global ionospheric convection map from the SuperDARN data because individual radars give only line-of-sight components of plasma drift velocity and the data are frequently missing. In our technique, the plasma velocity distribution is represented by a sum of divergence-free spherical elementary current systems, which provides a constraint ensuring the divergence free condition. In this paper, we will demonstrate a preliminary results obtained by our newly developed method.

Keywords: ionospheric convection, SuperDARN, spherical elementary current systems

Reconstruction of Plasmaspheric Density Distributions by Applying a Tomography Technique to Jason-1 plasmaspheric TEC Measurements

*Eunsol Kim[1], Yongha Kim[1], Geonhwa Jee[2]

1. Chungnam National University, 2. Korea Polar Research Institute

GPS receiver onboard Jason-1 satellite provides the measurements of plasmaspheric total electron content (pTEC) between the altitudes of Jason-1 and GPS satellites (1,336 and 20,200 km, respectively). We developed a tomography algorithm and applied it to the Jason-1 pTEC data to reconstruct the plasmaspheric density distributions. To invert the observed pTECs into the vertical distribution of plasmaspheric electron density, we adopted a multiplicative algebraic reconstruction technique (MART) with an initial density from *Huang et al. (2004)*. The reconstruction of the plasmaspheric density distribution was performed on Indian ( ), Pacific ( ), and Atlantic ( ) longitudinal planes during the periods of high solar activity ( ) and low geomagnetic activity ( ) from 2002 to 2005. It is found that the reconstructed density distribution displays general climatological characteristics of the plasmasphere. For all three longitudinal sectors, the reconstructed distributions show weak diurnal variations being greater during daytime (09 –15 LT) than nighttime (21 –03 LT). In the Atlantic sector, the reconstructed plasmaspheric density exhibits an annual anomaly (higher density in December than in June), while it was not apparent in the other longitude sectors. By fitting the reconstructed density profiles, we derived the empirical profiles of equatorial plasmaspheric density for four seasons (March, June, September, and December) and for three longitude sectors. The empirical profiles display the diurnal variation and the annual anomaly, and significantly differ from those obtained from other kinds of plasmaspheric measurements.

Keywords: Plasmasphere, Tomography, Total Electron Content, GPS

Latitudinal and Longitudinal Profile of EEJ current during different phases of Solar Cycle

*Nurul Shazana Abdul Hamid[1], Wan Nur Izzaty Ismail[1], Mardina Abdullah[2,3], Akimasa Yoshikawa[4]

1. School of Applied Physics, Faculty of Science and Technology, Universiti Kebangsaan Malaysia, 43600 UKM, Bangi, Selangor, Malaysia, 2. Space Science Centre (ANGKASA), Institute of Climate Change, Universiti Kebangsaan Malaysia, 43600 UKM, Bangi, Selangor, Malaysia, 3. Department of Electrical, Electronic and Systems Engineering, Faculty of Engineering and Built Environment, Universiti Kebangsaan Malaysia, 43600 UKM Bangi, Selangor, Malaysia, 4. International Center for Space Weather Science and Education (ICSWSE), Kyushu University 53, 6-10-1 Hakozaki, Higashi-ku,Fukuoka 812-8581,Japan

Study of equatorial electrojet (EEJ) has always been one of the research interest in ionospheric field. EEJ current is an eastward current that flows within the range of ±3˚ at dip equator. In this study, we attempt to find the latitudinal and longitudinal profile of this ionospheric current. This research is carried on using data from magnetometer network from Magnetic Data Acquisition System (MAGDAS)/ Circum-pan Pacific Magnetometer Network (CPMN), Indian Institute of Geomagnetism (IIG) and International Real- Time Magnetic Observatory Network (INTERMAGNET). The analysis is carried out using geomagnetic northward H component which is later used to calculate the magnetic component of EEJ. In order to correct the latitudinal effect causes by the location of observatories, we applied the normalization technique of observation data. The EEJ latitudinal profile is obtained and it shows that the current started to reverse westward at 5˚ latitude and not more than 10˚ latitude in both hemispheres. On the other hand, the longitudinal profile obtained shows that EEJ is higher in American sector and lowest between African and Indian sector in solar minimum (2008) and inclination phase (2011) of solar cycle. However, in solar maximum (2014), the EEJ current is found to be comparable between American and Southeast Asian sector. Moreover, our result agreed with previous study, showing that the Sq current does not vary with longitude, especially in solar minimum.

Keywords: Equatorial electrojet, Latitudinal profile, Longitudinal profile, Solar cycle

The Sq-current and the Ionospheric Profile Parameters during Solar Minimum

*Nurul Shazana Abdul Hamid[1], Saeed Abioye Bello[2,4], Mardina Abdullah[2,3], Akimasa Yoshikawa[5]

1. School of Applied Physics, Faculty of Science and Technology, Universiti Kebangsaan Malaysia, 43600 UKM, Bangi, Selangor, Malaysia., 2. Space Science Centre (ANGKASA), Institute of Climate Change, Universiti Kebangsaan Malaysia, 43600, UKM Bangi, Selangor, Malaysia, 3. Department of Electrical, Electronic and Systems Engineering, Faculty of Engineering and Built Environment, Universiti Kebangsaan Malaysia, 43600 UKM Bangi, Selangor, Malaysia. , 4. Faculty of Physical Sciences, Department of Physics, University of Ilorin, Nigeria, 5. International Center for Space Weather Science and Education (ICSWSE), Kyushu University 53, 6-10-1 Hakozaki, Higashi-ku, Fukuoka 812-8581, Japan.

The bottomside electron density profile of ionospheric F2-layer can be described by the peak electron density (NmF2), maximum height of F2-layer (hmF2), bottomside thickness (B0) and shape (B1) parameter. We analyze simultaneous quiet days records of these profile parameters with the solar quiet of geomagnetic H-component (SqH) that was obtained from the Peruvian and Ilorin stations respectively during solar minimum. We observe a midday peak in hmF2 and B0 for all the months under study. At the Peruvian station, a post-sunset peak in hmF2 and B0 during the equinoctial month was observed. For all the seasons, we observe peaks in NmF2 during the midday and post-noon periods. The results further show that the variation in SqH current is mainly responsible for that in hmF2 and B0. Both NmF2 and B1 are observed to be less sensitive to the variations in the Sq-current.

Keywords: Ionosphere, Electron density profiles, Sq-current

The correlation analysis of ionospheric characteristics and the geomagnetic Sq fields

*Yu-Jung Chuo[1]

1. Department of Information Technology, Ling Tung University

This study is trying to analysis variations of ionospheric characteristics and geomagnetic Sq fields. Using hourly data of the H and Z components of the geomagnetic observatories from mid-latitudes to equator over the eastern Asian sector in 1999, to calculate the Sq current. The other hand, we calculated the ionospheric total electron content (TEC) by using global positioning satellite system (GPS) data in 1999. In this investigation, we show the daily, seasonal and annual variations of geomagnetic Sq fields and TEC during the solar quiet period in 1999. Meanwhile, this study also collects ionosonde data in Chung-Li at Taiwan to analysis the cross correlation and discussion the possible physics processes for the variation of ionosphere corresponding to the geomagnetic Sq fields.

Keywords: ionospheric dynamo, geomagnetic field, Sq current

Observation of auroral brightenings and fast plasma flows produced by magnetic reconnection in the magnetotail

*Kawashima Takahiro[1], Akimasa Ieda[1], Miura Tsubasa[1]

1. Institute for Space-Earth Environmental Research

Substorm is explosive release of energy that is stored in the magnetotail and is manifested by explosive auroral brightenings. According to the reconnection model of substorm, the stored magnetic energy is converted to the plasma energy by the magnetic reconnection at about 20 Re down the tail. This magnetic reconnection creates a pair of earthward and tailward fast plasma flows. The earthward plasma flows are supposed to hit the inner magnetosphere at 10 Re down the tail, leading to explosive auroral brightenings (i.e., substorm onset). Thus, fast plasma flows are expected at 10 Re and beyond at the times of substorm onsets. To demonstrate this expectation, in this study we investigated fast flow produced by magnetic reconnection, using multi-satellite observations of the tail and ground all-sky images. Thus, we investigated this reconnection event with fast tailward flow.
At 06-07 UT February 27, 2009, each of THEMIS satellites were located near midnight 21 Re (THEMIS-1), 18 Re (THEMIS-2) and 11 Re (THEMIS-3, 4, 5) down the tail. Satellite foot-points were located near Gillam (magnetic latitude: 66.0 degree) in Canada. An auroral brightening started at 0636:00 UT (23.5 MLT) with ray structure. At this time, THEMIS-1 observed tailward fast flow at 21 Re. In addition, THEMIS-3, 4 observed earthward fast flow at 11Re. In contrast, THEMIS-2 did not observed fast flow. Since the plasma beta was decreasing at this time, THEMIS-2 moved toward the tail lobe. These THEMIS 2 observations suggest that no fast flow was observed at 18 Re because the plasma sheet was thinning.

Keywords: aurora, substorm, magnetic reconnection

Auroral intensification in relation to the magnetotail Pi2 and EMIC wave enhancements

*Tohru Sakurai[1]

1. Tokai University

This paper presents an important observation for an auroral intensification event in strong relation to the magnetotail Pi 2 and EMIC wave enhancements observed during a substorm event on 04 April 2009. Substorm onset was identified at 08:32 UT with an auroral initial brightening and then an initiation of Pi 2 oscillations at 08:26 UT. About 6 minutes after the auroral intensification occurred at 08:32 UT. The Pi 2 and EMIC wave enhancements were observed at the same time, when THEMIS B satellite encountered the dense plasmaspheric plume at X=~7~8 Re, where was far from the usual location of the plasmapause boundary in the mid-night magneotail. The generation of the EMIC waves was found to be in association with the newly injected westward-drifting ions, oscillating with Pi 2 period. Wave modes appeared with electro-acoustic modes signifying ordinary sound wave, slow mode wave and electromagnetic ion-cyclotron (EMIC) waves at the same time. The frequency of these waves was found to be near He+ gyro-frequency, implying that the presence of heavy ion (He+) might provide new couplings (instabilities) for these EMIC waves. The generation of the EMIC waves might drive the electron heating, suggesting an important candidate for auroral intensification electrons, within the overlap of the ring current and the plasmasplume through some mechanisms such as Coulomb collisions of plasmaspheric electrons with the ring current ions, Landau damping of electromagnetic ion cyclotron waves generated by ring current ions, and/or kinetic Alfven waves in association with the waves. Another important result obtained in this study is a finding of good conjunction between the ground station and the magnetotail from the observation of Pi 2 oscillation period and phase relations between them. The velocity field oscillations observed at the THEMIS-B in the magnetotail showed a same oscillation period of Pi 2 observed on the ground. The velocity field Pi 2 oscillation at the magnetotail leads a quarter cycle for the Pi 2 oscillations observed on the ground. These observations imply that the generation of field-aligned currents (FAC’s) in association with the velocity field oscillations in the equatorial plane might establish the field-line resonance for these Pi 2 oscillations. Therefore, the present study provides the important role of Pi 2 and EMIC waves for auroral intensification and certifies a good conjugacy between the ground station and the satellite location in the magnetotail.

Keywords: aurora, magnetosphere, electro-magnetic waves, Pi 2 magnetic pulsation, electro-magnetic ion cyclotron wave, plasmapause

Comparison of substorm onsets between all-sky images and Pi2 magnetic pulsations.

*Miura Tsubasa[1], Akimasa Ieda[1], Kawashima Takahiro[1]

1. Institute for Space-Earth Environmental Research (ISEE), Nagoya University

Substorms are explosive disturbance in the earth’ s magnetosphere and ionosphere. Substorm onset are traditionally identified using sudden auroral brightenings or magnetic Pi2 pulsations. These auroral brightenings and Pi2s are believed to occur typically within 1 minutes. On the other hand substorm onset has originally been defined to have two-stage development, i.e., two brightenings. Thus, it is unclear whether the Pi2s correspond to the first or the second brightening. To clarify this association, we compared all-sky images and Pi2 pulsations in Canada, using the data from THEMIS project. As a result, a Pi2 pulsation was observed at 04:36 UT on 29 February 2008. About the same time, an auroral initial brightening (04:33:30 UT) and the poleward expansion (i.e., the second brightening, 04:39:18 UT) were observed in Fort Smith. This result suggests that the Pi2 pulsation can be delayed by a few minutes from the substorm onset, which is originally defined by the auroral initial brightening.

Keywords: All-Sky Images (ASIs), auroral breakup

Simultaneous existence of the cusp aurora and polar cap arcs during northward IMF

*Yushin Oda[1], Satoshi Taguchi[1], Keisuke Hosokawa[2]

1. Graduate school of science, Kyoto University, 2. Department of Communication Engineering and Informatics, University of Electro-Communications

The cusp aurora for northward IMF is created by the particle precipitation caused by high-latitude reconnection poleward of the cusp. The aurora generally appears at 75 - 80 MLAT in the daytime sector. In this sector the polar cap arcs are also often seen when IMF is northward. In this research we show the spatial and temporal features of the cusp aurora and polar cap arcs by examining events in which both exist simultaneously. We analyzed the 630 nm auroral image data from a highly sensitive all-sky imager at Longyearbyen, Svalbard in Norway, and the precipitating particle and ion drift data from the DMSP spacecraft. The spacecraft data show that lobe convection exists in the daytime sector, and that the cusp electron precipitation and higher-energy electron precipitation occur at different places simultaneously. It is also clear from the all-sky image data that the former and latter produce the cusp aurora and polar cap arcs, respectively. Detailed examination of the all-sky image data obtained immediately before and after the time when whether the observed auroral structures are the cusp proper or polar cap arcs are undoubtedly determined reveals their spatial and temporal features.

Keywords: cusp aurora, northward IMF, polar cap arcs

Study of polar cap potential saturation using global MHD simulation: Difference between steady and unsteady state

*Yasubumi Kubota[1], Tsutomu Nagatsuma[1], Mitsue Den[1], Shigeru Fujita[2], Aoi Nakamizo[1], Takashi Tanaka[3]

1. National Institute of Information and Communications Technology, 2. Meteorological College, 3. Kyushu University

The cross polar cap potential (CPCP) is a value of the convection cycle strength of a solar wind-magnetosphere-ionosphere (SW-M-I) system via Region-1 FAC. CPCP shows an almost linear relationship with the solar wind merging electric field, but it tends to be saturated when the merging electric field becomes large. Siscoe et al. [2002], by using global MHD simulation, suggested that the CPCP basically depends on solar wind electric field, dynamic pressure and ionospheric conductivity. They also suggested that CPCP saturation results from the fact that the solar wind dynamic pressure limits the amount of Region-1 FAC. Their discussion is based on steady state of simulation results, however, in actual cases, solar wind and ionosphere conductivity vary with time and accordingly the state of SW-M-I system should be changed. The purpose of this study is to investigate the cause of the CPCP saturation for time varying condition. In this presentation we will discuss the difference of CPCP saturation between steady and unsteady states.

Possible Formation Mechanism of “Reverse L”-Shaped Transpolar Arc and Associated Ionospheric Flows: A Multi-Event Study

Jun Yang[1], *Motoharu Nowada[1], Quan-Qi Shi[1], Robert C. Fear[2], Adrian Grocott[3]

1. Center for Space Weather Sciences, Institute of Space Science, School of Space Science and Physics, Shandong University at Weihai, 2. Department of Physics and Astronomy, University of Southampton, 3. Space and Planetary Physics Group, Department of Physics, Lancaster University

We found six events of the interesting shape of Transpolar Arc (TPA) among a large database of IMAGE and POLAR during 5 years between 2000 and 2005. The two events out of six events were observed in northern hemisphere, and the rests were seen in southern hemisphere. A shape of the observed TPA was just like a reversal of the alphabetical letter of “L”, that is, a part of the nightside end of the TPA is “bending” toward the midnight sector. The “bending” polar arc, which is only growing from the nightside main auroral oval, is well-known as “bending arc”, but the TPA, having a bending part at the nightside end, completely grew toward the dayside auroral region. When this “Reverse L”-shaped TPA was observed, the B_z component of the Interplanetary Magnetic Field (IMF) was dominantly northward in almost of cases, and the TPA’s location was determined by the orientation of the IMF-B_y component; the dawn(dusk)side of TPA in northern (southern) hemisphere was seen during the negative B_y component, and under the positive B_y component, the TPA was observed in dusk(dawn)side in northern (southern) hemisphere, which are consistent with the result of a statistical survey for the TPA locations as reported previously. Particularly, on the “Reverse L”-shaped TPA event observed in the northern hemisphere on 22, September, 2000, the SuperDARN radar had detected the ionospheric fast flows, whose range was larger than 0.7 km/s, on the pre-midnight sector of the main auroral oval since, at least, about 2 hours prior to the TPA appearance. Even during the “Reverse L”-shaped TPA brightening, these fast flows persisted. These plasma flows seen in the ionosphere are identified as ionospheric fast flows associated with “Tail Reconnection during IMF Northward Non-substorm Intervals (TRINNIs)”, supporting that this interesting TPA would be formed by nightside magnetic reconnection. However, we also found the case where the TPA separated into the dayside and nightside parts after its appearance, that is, the middle part of the TPA had a “void” structure. These characteristic signatures on the TPA might suggest that formation of “Reverse-L”-shaped TPA would not be addressed by the nightside magnetic reconnection model alone.
We have proceeded further in analysis of these interesting “Reverse L”-shaped TPA events based on both ground- and space-based observations, and supportive global MHD simulations. In this paper, we will discuss the features of ionospheric TRINNI’s flows, whose triggering mechanism is suggestive of nightside magnetic reconnection, and a possible formation mechanism of the “Reverse L”-shaped TPAs based on the results obtained through the detailed analyses.

Keywords: Transpolar Arc, Magnetotail Reconnections, Ionospheric Flows, TRINNIs

Field line dipolarization and currents in the ionosphere: A case study

*Osuke Saka[1]

1. Office Geophysik

Ionospheric current associated with the field line dipolarization event (1200 UT, 10 August 1994) is studied using ground magnetometer data of 30 ground stations from Alaska, Alberta, Manitoba and to Labrador, as well as using plasma measurements from LANL geosynchronous satellite at the Alaskan sector. Results from the ground magnetometer data are as follows:

(1) On the ground, there appeared inflection points in the latitudinal profiles of the vertical component. This finding infers that the peak of the ionospheric currents, either eastward or westward, existed at the latitudes of the instantaneous inflection points.

(2) In the first ten to fifteen minutes of the dipolarization onset, the most poleward inflection point moved in latitudes rapidly from 68N to 75N. The Pi2 amplitudes in auroral zone exhibited the largest ones (40nT peak-to-peak).

(3) After the poleward inflection point has reached to 75N, the inflection point to the south, corresponding to Westward Electrojet, shifted from 65N to 68N. The Pi2 amplitude reduced to halve.

(4) The inflection point in the southernmost latitudes, though no significant motion in latitudes was observed, disappeared in one hour after the onset.

(5) During a rapid expansion of the most northward inflection point, the downward FACs were observed in the eastward sector of the onset. They propagated eastward away from the onset longitudes.

The present ground magnetometer observations support the results from the in situ plasma measurements at geosynchronous orbit that the field line dipolarization is composed of the parallel shrinkage along the field lines and simultaneous perpendicular stretching in dawn-dusk direction.

Keywords: Field line dipolarization, Ionospheric current, M-I coupling

Ionospheric Aflvén resonator observed at low-latitude ground station

*Masahito Nose[1], Makoto Uyeshima[2], Jun Kawai[3], Hideaki Hase[4]

1. Graduate School of Science, Kyoto University, 2. Earthquake Prediction Research Center, The University of Tokyo, 3. Applied Electronics Laboratory, Kanazawa Institute of Technology, 4. Geothermal Energy Research & Development Co., Ltd.

The ionospheric Alfvén resonator (IAR) is found in dynamic power spectrum of the geomagnetic field variations as spectral resonance structures in the frequency range 0.1–10 Hz. The first observations of IAR were reported by Belyaev et al. [1989, 1990] by using induction magnetometers installed at a mid-latitude station, Gorkii (L~2.65). Since then, studies of IAR have been focused on events at mid and high latitudes. To date, observations of IAR at low latitude are only made at Crete by Bösinger et al. [2002, 2004] and not sufficient enough to reveal its general characteristics. We therefore installed an induction magnetometer at Muroto, Japan (24.40° geomagnetic latitude, −155.56° geomagnetic longitude), in December 2013 to investigate low latitude IAR in greater detail. Its dipole L value is 1.206 and smaller than that of Crete (L~1.3). Cadence of observations is 64 Hz. We analyze data from the induction magnetometer for the period from 28 December 2013 to 13 August 2016. From the statistical analysis of IAR observed at Muroto, we find that its occurrence probability is (1) dominant during nighttime with a gradual increase from the dusk sector to midnight and a broad maximum at 00–05 LT followed by a sudden decrease at the dawn sector, (2) slightly higher during May through September (in summer and fall), and (3) independent to the Kp index. We also find that (4) IAR at Muroto has frequency separation between the harmonics (Δf) of 0.1–0.5 Hz with a peak at 0.200–0.275 Hz. It has been considered that IAR is caused by Alfvén waves trapped in the ionospheric cavity bounded by the conductive E layer and a steep gradient of Alfvén velocity above the F2 layer. We calculate the resonant frequency and the Q factor of the ionospheric cavity, using analytical equations proposed by Polyakov and Rapoport [1981] with the IRI-2012 and IGRF-12 models. Results of comparison between the observations and the model calculation will be discussed.

Spatiotemporal variation of precipitating electron energy in auroral vortices

*Yoshimasa Tanaka[1], Yasunobu Ogawa[1], Akira Kadokura[1], Kirsti Kauristie[2], Carl-fredrik Enell[3], Urban Braendstroem[4], Tima Sergienko[4], Bjorn Gustavsson[5], Daniel Whiter[6], Alexander Kozlovsky[7], Hiroshi Miyaoka[1], Mike Kosch[8]

1. National Institute of Polar Research, 2. Finnish Meteorological Institute, 3. EISCAT Scientific Association, 4. Swedish Institute of Space Physics, 5. The Arctic University of Norway, 6. University of Southampton, 7. Sodankyla Geophysical Observatory, 8. South African National Space Agency

We investigated dynamic vortex structures in discrete arcs observed by multi-point monochromatic (427.8nm) imagers in Northern Europe at 22:15-22:20 UT on March 14, 2015. We applied auroral computed tomography method to the multiple images taken at 2 second interval by three all-sky EMCCD imagers and at 5 second interval by four wide-view CCD imagers, and reconstructed a 3D distribution of auroral emission and a horizontal 2D distribution of energy of precipitating electrons. The reconstructed 3D distribution of the auroral emission was compared with height profiles of ionospheric electron density along a field line simultaneously observed by EISCAT UHF radar at Tromso, Norway.
The analysis results are summarized as follows. (1) Averaged energy of auroral precipitating electrons was higher around the center of auroral vortices than the other location of the discrete arcs. (2) Total energy flux of precipitating electrons was proportional to the square of the averaged energy. (3) The shape of height profiles of the 427.8nm emission was very similar to that of the electron density profiles. (4) The electron density estimated from the 427.8nm emission by using empirical atmosphere models was about 2.5 to 3 times smaller than observed by EISCAT UHF radar. The result (1) is consistent with the Ohm’s law along a field line, i.e., the field-aligned current (FAC) is proportional to the field-aligned potential difference. If the discrete arcs were caused by electron precipitation from the auroral acceleration region (AAR) where the Ohm’s law is satisfied, the electron energy (proportional to the potential difference) should have been high around the center of vortex where FAC is large. The result (2) strongly supports this inference. As for the item (4), the difference between the electron density estimated from the optical emission and that observed by EISCAT radar may be explained by an uncertainty of some atmospheric parameters derived from empirical models, in particular, an effective recombination coefficient. We discuss the dynamics of the auroral vortices in terms of the magnetosphere –ionosphere coupling.

Keywords: auroral vortex structure, precipitating electron energy, tomography analysis, EISCAT radar, magnetosphere - ionosphere coupling

The estimation of spatial structures of magnetospheric plasma by using the data observed by LEO satelites.

*Yoshihiro Yokoyama[1], Toshihiko Iyemori[2], Tadashi Aoyama[1]

1. Department of Earth and Planetary Sciences, Graduate School of Science, Kyoto University, 2. Data Analysis Center for Geomagnetism and Space Magnetism,Graduate School of Science, Kyoto University

In the regions of high-beta plasma such as the plasma sheet or the boundary layer in the magnetosphere, it can be expected that the plasma behaves as turbulence due to the effects of various plasma instabilities, non-linear development of Alfven waves, and so on. Satellites in the plasmasheet also have observed the fluctuations in velocity and magnetic field that have the characteristics of fluid turbulence (Borovsky et al. 1997). If the plasmas usually behave as turbulence, the spectrum and their distribution are important for understanding phenomena in the magnetosphere. However, it is almost impossible to have sufficient simultaneous satellite observations that cover the huge magnetospheric domain.

On the other hand, we confirmed that the magnetic fluctuations having period longer than 2s observed by low Earth orbit (LEO) satellites can be regarded as the manifestation of the spatial structure of the field-aligned currents by using the magnetic data obtained by Swarm satellites during December, 2013 when the satellites flew on nearly the same orbits with slight time separations. In addition, the LEO satellites fly through wide range of magnetic latitudes in a short period of time, so, by project- ing their orbits into the magnetosphere, they can scan wide range on the equatorial plane of the magnetosphere. therefore, by projecting these fluctuations onto the equatorial plane of the magnetosphere, i.e., the source regions of field-aligned currents, we try to estimate the distribution of turbulent region and their characteristics there.

We made statical maps of the amplitude of magnetic fluctuations for both quiet(AE<50nT) and disturbed(AE>50nT) conditions. We also made spectral analysis of magnetic fluctuations by MEM and found that there are many peaks in wide frequency range in every spectrum regardless of the geomagnetic conditions, MLTs, and so on.

This result suggests that the magnetospheric plasmas usually behave as turbulence.
In this paper, in addition to the result above, we also discuss the wave-number spectrum in the magnetosphere.

Keywords: SWARM satellite, magnetospheric plasma

Ground-based and magnetospheric observation of auroral finger-like structures using the RBSP-A satellite in the inner magnetosphere

*Katsuki Nishi[1], Kazuo Shiokawa[1]

1. Institute for Space-Earth Environmental Research, Nagoya University

Auroral emissions are caused by electron precipitation from the magnetosphere along Earth’s magnetic field, and project the magnetospheric plasma dynamics onto the ionosphere. The knowledge of plasma dynamics acquired from investigation of auroral structures is important for future space developments. In our previous research, we reported first conjugate observation event of auroral finger-like structures using the THEMIS GBO cameras and the THEMIS satellites, which was located at radial distance of ~9 Re in the dawnside plasma sheet. The auroral finger-like structures appears in the equatorwardside of the auroral oval in diffuse auroral region, and contribute to the auroral fragmentation into patches mainly during substorm recovery phase. In this study, we searched simultaneous observation events of auroral finger-like structures using the RBSP satellites which has an apogee of 5.8 Re in the inner magnetosphere. The best event which we found is that observed at Gillam, Canada, at ~0900 UT on 14 Nov. 2014. In this event, the footprints of the RBSP-A satellite passed across the auroral finger-like structures several times according to the field-line mapping using the Tsyganenko-01 magnetic field model. We obtained observational facts from this simultaneous observation event as: 1) both electron and ion OMNI fluxes measured by HOPE increase at ~0900 UT as the satellite footprint was getting into the auroral region; 2) electron cyclotron harmonics (Ech) wave activities at ~1 kHz measured by EMFSIS enhanced after 0900 UT; 3) electric field in GSM-Y direction measured by EFW decreases during northward development of the finger-like structures; 4) absolute value of magnetic pressure is almost ten times larger than that of ion thermal pressure; 5) variation of magnetic pressure and ion thermal pressure are seen in various time scales, including ~5 min which is the time scale of crossing of finger-like structures. In the presentation, we will discuss these observations in the context of magnetospheric instabilities that can cause auroral finger-like structures.

Keywords: auroral finger-like structure, RBSP, inner magnetosphere

Proton aurora dynamics by spectroscopic observations at geomagnetic conjugate points

*Yuki Takahashi[1], Makoto Taguchi[1], Akira Kadokura[2]

1. Rikkyo University, 2. National Institute of Polar Research

Even the brightest proton aurora (486.1nm) is far weaker than electron auroras. When proton aurora is observed, strong emissions from nitrogen molecular ions excited by precipitating electrons may be a contamination. This is the reason why few conjugate observations of proton aurora have been conducted. The studies of proton aurora dynamics using monochromatic imagers in the past could not be definitively justified, because the contamination might remain after subtracting background emission simultaneously observed at a wavelength close to from the image. In this study a spectrum in a wide wavelength range that includes the wavelength of proton aurora is obtained by a proton aurora spectrograph (PAS) in order to precisely eliminate the background emission by electron auroras. PAS has a narrow field-of-view of 180˚ along a geomagnetic meridian, which is accomplished by a variable-width slit placed at the focal plane of an all-sky optics. Light that passes through the slit is converted to a parallel beam and fed into a transmission diffraction grating. Then a space vs wavelength image is projected on a CCD with 1024 × 1024 pixels. Pixel counts are increased by 2 ×2 pixel binning. PAS is designed to observe a wavelength range from 417 nm to 579 nm with a spectral resolution of 2 nm. PAS was installed at the optical observation site at Tjornes in Iceland in early September 2016. Continuous observation started on September 27, 2016, and will end on April 26, 2017. An image was obtained every 3 min with an exposure time of 177 sec from September 27, 2016 to December 8, 2016 and every 1 min with an exposure time of 55 sec from December 12, 2016. The difference in the exposure time is due to increase of sensitivity by updating the CCD camera. The slit width is set to be slightly wider than the designed value, and moreover it is not constant with the zenith angle. Therefore, the slit will be adjusted or replaced to increase the spectral resolution so that the background emission can be perfectly eliminated before the next observation season. An identical system will be developed in early 2017, and will be installed at Syowa Station, where is the geomagnetic conjugate point of Tjornes, during the 2017/2018 summer season. Then conjugate observations of proton aurora will be started from the spring season in 2018.
An example of the spectral data obtained from September 27, 2016 to April 26, 2017 will be introduced and discussed in the presentation.

Development of automatic detection and tracking technique for pulsating aurora

*Takumi Inoue[1], Tomohiro Inoue[2], Mitsunori Ozaki[3], Satoshi Yagitani[3], Kousuke Imamura[3]

1. School of Electrical and Computer Engineering, Kanazawa University, 2. Graduate School, Kanazawa University, 3. Institute of Science and Engineering, Kanazawa University

Pulsating aurora is a kind of aurora blinking with several tens of seconds period and having a patchy structure with several to hundreds of kilometers spatial scale. It is difficult to automatically detect pulsating aurora in a video image because the spatial and temporal features of pulsating aurora are complex. Then, statistical analysis would not be enough due to the difficulties. In this study, in order to perform the statistical analysis of pulsating aurora, we have developed an automatic detection and tracking technique for pulsating aurora. Pulsating aurora usually appears simultaneously with diffuse aurora. We apply Low Pass Filter to the brightness variations to reduce the effect of diffuse aurora. Then, we use the Level Set Method to detect the outer shape of pulsating auroral patches. However, the aurora images include a lot of noise so that we are not able to accurately extract pulsating aurora. Here, we evaluated two noise reduction techniques. First is enhancement of the brightness values of aurora images by using a nonlinear function to compress the noise. Second is using the spectral entropy, which is a signal processing method for classifying signal and noise. As a result of evaluation using test data, the first method showed lower error rate of detection (less than 10%) at a signal-to-noise ratio of -5 dB or more in comparison with the second method. We track the motion of pulsating aurora by using a particle tracking technique. We evaluate the accuracy of the tracking technique with a test movie including a simulated auroral patch. The result showed that the tracking error was less than 1 pixel at the signal-to-noise ratio of -10 dB or more.
In this presentation, we will discuss our automatic detection and tracking method for pulsating aurora in detail.

Keywords: Pulsating aurora, Image processing technique, Level Set Method

Characteristics of pulsating aurora modulation observed from high-speed EMCCD camera

*asano takaki[1], Yoshizumi Miyoshi[1], Satoshi Kurita[1], Shin-ichiro Oyama[1], Keisuke Hosokawa[2], Yasunobu Ogawa[3], Takanori Nishiyama[3], Shinobu Machida[1]

1. Institute for Space-Earth Environmental Research, ISEE, Nagoya University., 2. Department of Communication Engineering and Informatics, University of Electro-Communications, 3. National Institute of Polar Research

Pulsating aurora (PsA) shows quasi-periodic intensity modulation with a 2 s to 30 s intervals as a main modulation. PsA is mainly observed from the post-midnight to the morning sectors during the recovery phase of substorms. PsA consists of not only main modulations but also internal modulation with a few Hz. We installed multi-EMCCD cameras in Tromso, Finland, Sodankyla, Kevo Finland and Alaska, US. The cameras with RG665 filters observe high-speed phenomena with 100 Hz sampling rate, while the cameras with different filters observe spectrum of PsA with 10 Hz sampling rate. In order to investigate spatio-temporal characteristics of the main modulations as well as internal modulations, we apply PCA (Principal Component Analysis) and FFT to all-sky images of PsA with 100 Hz sampling rate. PCA decomposes into different modes with periods of a few seconds, indicating that localized structure of the main modulation of PsA. The all-sky images at different frequency derived from FFT show that the spatial distribution of PsA depends on the frequency and the internal modulations with high frequency appear in a part of the main modulations. In this presentation, we will report statistical results on these spatio-temporal characteristics of PsA.

Keywords: aurora

Coordinated EISCAT and optical network imaging observations of the omega-band type pulsating aurora and electron density enhancement in the D-region ionosphere

Hirona Kondo[1], *Takeshi Sakanoi[1], Yasunobu Ogawa[2], Yoshimasa Tanaka[2], Kirsti Kauristie[3], Brändström Urban[4], Björn Gustavsson[5], Masato Kagitani[1]

1. Planetary Plasma and Atmospheric Research Center,Graduate School of Science,Tohoku University, 2. National Institute Polar Research , 3. Finnish Meteorological Institute, Finland, 4. Swedish Institute of Space Physics, Sweden, 5. UiT The Arctic University of Norway, Tromsø, Norway

We report the coordinated EISCAT and optical observations for omega-band type auroral events.
Omega band and torch auroral structures are characterized by large-scale wavy forms appeared at the poleward boundary of a diffuse aurora mainly in the post-midnight and morning sectors, and pulsating auroral patches are often observed inside the structure. Past studies revealed that pulsating aurora is caused by relatively high-energy (greater than 10 keV) electrons. However, the precise characteristics of precipitating electrons associated with omega-band and torch auroras have not been understood well. We estimated the emission height of pulsating aurora appered with omega-band and torch structures from triangulation with multiple all-sky imaging data, and the energy distribution of precipitating electrons from EISCAT radar data.
We carried out coordinated observation of omega-band aurora with the EISCAT Tromso UHF radar and MIRACLE all-sky imagers at Kilpisjarvi, Abisko and Tromso with high spatiotemporal resolution at 01:00-02:00 UT (03:30-05:30 MLT) on 6 January and 01:00-02:00 UT (03:30-05:30 MLT) on 13 January, 2016. We obtained the time variation of emission heights for 427.8nm auroras using the triangulation. The results showed that 427.8nm emission height of omega-band aurora was 92-98 km at 6 January and 90-112km at 13 January.
Furthermore, we obtained the time variation of energy fluxes of precipitation electrons for energy bands, i.e., 1-4 keV, 4-10 keV, 15-50 keV, 60-100 keV and 110-170 keV. We found that the electrons with energy up to 100 keV precipitated in the vicitnity of omega-band and torch aurora at 01:00-01:15 UT on event1. On other hand, 15-50 keV electrons were dominant to produce the omega-band aurora at 01:20-01:40 UT on 13 January, and its energy spectrum was similar to that in the pulsating auroral patch at 01:15-01:30 UT on 6 January. Therefore it seems that that there are at least two types of generation mechanisms in the magnetosphere to produce precipitation electrons associated with pulsating patch inside of omega-band auroras. We consider that there are two region where wave-particle interaction occurs, one is the magnetic equatorial plane, the other is that resonance occurs widely from the equatorial plane to the high latitude side in the magnetosphere.
In addition, we quantitatively evaluated the estimation method of auroral emission height developed in this research. The result of the estimating emission height of discrete aurora and the difference between 427.8 nm and 557.7 nm auroral emission height were consistent with past studies. Furthermore, we investigated the positional relationship between the auroral spatial structure and the observation points for the pair of triangulation. Even if the auroral height estimation error is large using a pair of observation points, we found that it is possible to estimate the relatively probable emission height using the other pair. We also found the positive relationship between the electron density peak height estimated from EISCAT radar data and the emission height estimated with optical triangulation.

Keywords: Omega-band type aurora, EISCAT radar

Observation of auroral polarization using a polarization imaging spectrometer in Alaska

Reo Ono[1], *Takeshi Sakanoi[1], Masato Kagitani[1]

1. Planetary Plasma and Atmospheric Research Center, Graduate School of Science, Tohoku University

We aim to reveal the elevation distribution of auroral polarization along the magnetic meridian by using a wide field auroral polarization imaging spectrometer by observing auroral red line at OI 630 nm. We developed this instrument which consists of a fisheye lens, a wire grid type linear polarizer mounted on a rotating stage, a VPH transmission type diffraction grating and an EMCCD. It has a wide field-of-view of 130 degree covering the magnetic zenith and magnetic perpendicular, and its wavelength range is from 450 nm to 710 nm with a resolution of 2.0 nm. The polarization state of the incident light can be measured from the intensity change detected by the EMCCD when the polarizer is rotated by 45 degrees. In addition to auroral polarization, measurement data involve polarization effects due to atmospheric scattering, acrylic domes and optical system in the instrument (hereinafter referred to as instrumental polarization). Therefore, it is a key to carry out to obtain precise calibration data to correct the instrumental polarization. Although we have performed auroral polarization measurements since 2013, we got a problem in the calibration instrument and then did not obtain sufficient calibration data. In this study, we develop a new calibration instrument with a LED lamp monitoring the rotation angle of linear polarizer and succeeded to obtain the precise calibration data to correct the instrumental polarization. We also developed the data analysis method to apply the calibration data to measurement data to estimate the auroral polarization accurately.
We installed this instrument at Pokar Flat Research Range, Alaska in November of 2015 and took many calibration data for various field-of-view during our stay for about two weeks. As a result, calibration data with a quantitative accuracy better than 0.2 percent was obtained. Auroral polarization measurement continued till March of 2016. For a case of auroral polarization on November 19, 2015, the linear polarization degree of 630 nm aurora was 1.6 +/- 0.9 percent. For most cases, polarization degree showed a tendency that maximized at the low elevation angle toward the magnetic north, and decreases as the elevation angle increases. In addition, it showed that polarization degree increases again around the magnetic zenith toward the low elevation angle side in the magnetic south. We also obtained that the auroral linear polarization increases during auroral active period.

Keywords: aurora, polarization, spectroscopy

